A Survey With Numerical Assessment of Classical and Refined Theories for the Analysis of Sandwich Plates

E. Carrera[1]
Professor of Aerospace Structures and Applied Aeroelasticity
e-mail: erasmo.carrera@polito.it

S. Brischetto

Aeronautics and Space Engineering Department,
Politecnico di Torino,
Turin 10129, Italy

A large variety of plate theories are described and assessed in the present work to evaluate the bending and vibration of sandwich structures. A brief survey of available works is first given. Such a survey includes significant review papers and latest developments on sandwich structure modelings. The kinematics of classical, higher order, zigzag, layerwise, and mixed theories is described. An exhaustive numerical assessment of the whole theories is provided in the case of closed form solutions of simply supported panels made of orthotropic layers. Reference is made to the unified formulation that has recently been introduced by the first author for a plate/shell analysis. Attention has been given to displacements, stresses (both in-plane and out-of-plane components), and the free vibration response. Only simply supported orthotropic panels loaded by a transverse distribution of bisinusoidal pressure have been analyzed. Five benchmark problems are treated. The accuracy of the plate theories is established with respect to the length-to-thickness-ratio (LTR) geometrical parameters and to the face-to-core-stiffness-ratio (FCSR) mechanical parameters. Two main sources of error are outlined, which are related to LTR and FCSR, respectively. It has been concluded that higher order theories (HOTs) can be conveniently used to reduce the error due to LTR in thick plate cases. But HOTs are not effective in increasing the accuracy of the classical theory analysis whenever the error is caused by increasing FCSR values; layerwise analysis becomes mandatory in this case. [DOI: 10.1115/1.3013824]

1 Introduction

Sandwich structures are used to provide a stronger and stiffer structure for the same weight, or conversely lighter structures to carry the same load as a homogenous or compact-laminate flexural member. These structures are constituted by two stiff skins (faces) and a soft core, and they are widely used to build large parts of aircraft, spacecraft, ship, and automotive vehicle structures. Most of the recent applications have used skins constituted by layered structures made of anisotropic composite materials.

Many important issues should be considered in the design, analysis, and construction of sandwich structures, and these have been fully discussed in the well known books by Plantema [1], Allen [2], Zenkert [3], Bitzer [4], and Vinson [5] as well as in the handbook sections by Marshall [6] and Corden [7]. Among these issues, our interest is in comparing methods that are able to provide accurate evaluations of stress/strain fields in each layer in order to prevent failure mechanisms. Three-dimensional (3D) elasticity solutions (see Refs. [8–11]) could be used for this purpose. However, 3D solutions are difficult to obtain in the most general case of geometries and boundary conditions. The use of two-dimensional (2D) (plate and shell) models is preferred in most applications related to sandwich structures. 2D models are, in fact, more convenient than 3D ones in terms of required computational efforts. Various 2D models have been developed in literature over the past five to six decades. A summary of the general approaches can be found in the textbooks mentioned above. A relevant number of refined theories has been directed to improving the response of classical models based on the well known hypothesis by *Cauchy–Poisson–Kirchhoff–Love* [12–15] and by *Reissner–Mindlin* [16,17].

Significant increases in the development of refined theories have been caused by the advent of composite materials in aerospace structures. These materials are, in fact, according to their definition, made of multilayers. Their modeling involves the same complicated effects as a three-layered sandwich structure: First, composite materials show high transverse shear and normal deformability with respect to metallic ones. Second, the *zigzag* (ZZ) form of the displacement field in the thickness (transverse/vertical) directions (the displacement field shows a discontinuous slope at each layer interface) and the *interlaminar continuity* (IC) of transverse shear and normal stresses should be considered in refined models. ZZ and IC were referred to as C_z^0-requirements in Ref. [18]; that is, the displacement and transverse stress variables are C^0-continuous functions (piecewise) in the z-thickness direction, while their derivatives could be discontinuous at the interface. The textbooks by Lekhnitskii [19], Ambartsumian [20–22], Librescu [23], and Reddy [24] on multilayered structure modeling can be used to provide a review on available approaches versus refined models for layered structures.

Many survey articles have been published on sandwich and multilayered structure modelings. These include the reviews by Ambartsumian [25], Habip [26,27], Grigolyuk and Kogan [28], Sun and Whitney [29], Leissa [30], Librescu and Reddy [31], Grigolyuk and Kulikov [32], Kapania and Raciti [33], Kapania [34], Vasiliev and Lur'e [35], Noor and Burton [36,37], Burton and Noor [38], Noor et al. [39], Jemielita [40], Reddy and Robbins [41], Lur'e and Shomova [42], Grigorenko [43], Grigorenko and Vasilinenko [44], Altenbach [45], Librescu and Hause [46], Vinson [47], Carrera [48], Qatu [49], Hohe and Becker [50], and Hohe and Librescu [51]. A recent historical review on the so-called zigzag theories has been provided by Carrera [52]. The fundamental contributions by Lekhnitskii [53], Ambartsumian [54,55], and Reissner [56] were clearly outlined in this review work.

[1]Corresponding author.
Published online December 16, 2008. Transmitted by Assoc. Editor J. N. Reddy.

A unique and exhaustive classification of 2D models for layered/sandwich structures is difficult to make. An attempt is made below. The theories could be first distinguished according to the variable description in the layers. *Layerwise models* (LWMs) are those in which the number of variables is independent in each layer. Zigzag effects are intrinsically considered in LWMs. Interlaminar continuity cannot be a priori guaranteed by LWMs. *Equivalent single layer models* (ESLMs) preserve the numbers of the unknown variables independent by the number of constitutive layers. Zigzag and IC can be introduced into ESLMs, as has been described in Ref. [52]. Second, 2D theories can be distinguished according to the choice of the primary variables. If only displacements are used, the corresponding model can be referred to as *classical*, and the related models could be formulated on the basis of the principle of virtual displacements (PVD). If stresses are also employed as unknowns, the related models are referred to as *mixed* ones. Among the various mixed variational statements, Reissner's mixed variational theorem (RMVT), which was proposed in Ref. [56] and overviewed in Ref. [48], appears to be particularly suitable for multilayered structures since only transverse stresses are added to the displacements in order to fulfill IC.

Very often, the development of an improved theory is referred to as *a higher order theory* (HOT). In most cases these consist of refinements of the *classical lamination theory (CLT)* and *first order shear deformation theory* (FSDT) on which it is based.

The previously mentioned reviews are rather exhaustive. It should be noted that 817 papers were reviewed by Noor et al. [39], and 556 additional references were listed in the same papers. They considered almost all the work made in the past century. As a consequence, only a few papers that appeared in the past few years are considered in the following subsection to complete the survey given in the mentioned articles.

1.1 Brief Survey of Latest Developments. A relevant contribution on HOT for sandwich panels was given by Frostig and co-authors [57–61]. A transverse flexibly core was considered in Ref. [57] for bending problems. Multiskin and multilayered core constructions were addressed in Ref. [58]; the soft-core case was analyzed in Ref. [59]; localized effects in a nonlinear regime and soft core were considered in Ref. [60]. A section with an interesting literature survey on HOT was also given in this last paper. The extension to the core junction analysis has very recently been given in Ref. [61]. Pantano and Averill [62] considered the thermal stress analysis of sandwich plates in the framework of zigzag layerwise theories. The response to concentrated loadings using the higher order theory and 3D elasticity analysis was addressed by Swanson [63]; the assessment of the finite element modeling of the latter paper was provided in Ref. [64]. A local layerwise model for the bending of weak cores was presented by Whitney [65]. An assumed stress field in the thickness direction was assumed independently for the core and skins. The governing equations were obtained by referring to the stress method already used in the paper by Pagano [66]. The thick plate FSDT analysis was used by Liu and Zhao [67] for a comparison with a thin plate model analysis. The appropriate choice of shear correction factor was discussed by Birman and Bert [68]. Various HOTs were discussed by Matsunaga [69] for both sandwich and laminated plates. A finite element analysis of bended sandwich plates was considered by Topdar et al. [70], who employed an equivalent single layer (ESL) Ambartusumian-type theory. The already mentioned Frostig HOT was employed by Lyckegaard and Thomsen [71] to analyze the junction between flat and curved sandwich panels. A HOT finite element analysis for a free vibration of an anisotropic sandwich plate was conducted by Garg et al. [72]. A higher order approach for the vibration analysis of a sandwich plate with a viscoelastic core was proposed by Malekzadeh et al. [73] for the damping of local and global vibrations. Roque et al. [74] applied a layerwise theory based on radial basis functions to the vibration response of sandwich plates. Finally, various kinematics have recently been compared by Hu et al. in Ref. [75] for the analysis of sandwich beams made of viscoelastic materials.

1.2 The Numerical Assessment in This Work. In most of the available papers on sandwich structure modeling, such as those mentioned above, a proposed refined theory is only compared to an available 3D solution and/or to CLT/FSDT classical results. Only in very few cases is the comparison extended to other refined theories. This is, of course, an understandable limitation: HOT, in fact, gives CLT and FSDT results as particular cases, while the inclusion of further HOT analyses would require an additional implementation. On the other hand, it appears obvious that HOT will improve CLT/FSDT results and will not be any better than 3D analyses. This limitation does not offer the possibility of establishing the effective capability of a given HOT with respect to other available ones. From this point of view, it can be concluded that a complete numerical assessment of the most used refined and advanced theories for the static and dynamic analysis of sandwich structures would be welcome.

In the past few years, Carrera et al. [18,76–80] proposed a unified formulation (UF) of multilayered theories in the framework of both the PVD and RMVT applications. Classical models formulated on the basis of PVD and mixed models based on RMVT were both considered. LW and ESL models related to linear to fourth order expansion in the plate/layer thickness z-direction were implemented. ZZ, IC, transverse shear, and normal strain effects were addressed. Navier-type closed form solutions were obtained.

This paper reconsiders the above findings in order to provide a comprehensive numerical assessment of sandwich plate theories for the evaluation of both static and dynamic responses. Such assessment does not only review theories (that topic has been, in fact, largely covered by the mentioned survey articles): nevertheless this paper implements, thanks to UF, a large variety of plate theories by permitting a unique numerical comparison of them. That fact consists of the main contribution of the present "numerical survey" paper.

The following two parameters have been used in the analysis: a geometrical one, i.e., the length-to-thickness ratio (LTR), and a mechanical one, i.e., the face-to-core-stiffness ratio (FCSR). The various sandwich plate theories are compared, in terms of displacement, stress, and vibration response, with variations of LTR and FCSR. The following theories are all considered above: Classical theories (CLT and FSDT), HOT up to fourth order expansion in the thickness direction, HOT including Murakami's zigzag function (MZZF), layerwise analysis up to fourth order expansion in each layer, and mixed ESLM and LW theories based on Reissner's mixed variational theorem. Error with respect to a 3D solution is provided to establish the accuracy of a given analysis.

Classical, higher order, layerswise, and mixed theories are briefly described in Secs. 2–5. The results and discussions are provided in Secs. 6 and 7, while the conclusions are drawn in Sec. 8.

2 Classical Theories: CLT and FSDT

A large variety of plate theories have been considered in the present work in order to study how the various kinematic assumptions can affect the response of sandwich plates. A short discussion is given in what follows. A more detailed description of the used plate theories, including the explicit form of governing differential equations as well as the applied "closed form solution" technique, can be found in the already mentioned first author's work [80].

A plate of constant thickness h is considered. The geometry and reference system are shown in Fig. 1. x, y, and z are the Cartesian reference systems along whose directions the three displacement components u_x, u_y, and u_z are measured. z denotes the thickness direction, and Ω is the plate reference surface located in corre-

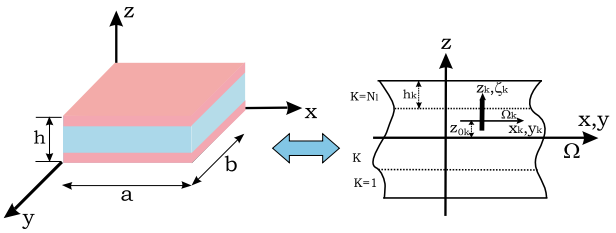

Fig. 1 Geometry and notations of the considered plate

spondence to the midplane of the plate. The plane stress/plane strain conditions have been imposed for all the considered theories according to the recent analysis reported in Ref. [81].

2.1 The Classical Lamination Theory. The CLT that is based on Cauchy- [12], Poisson- [13], or Kirchhoff-type [14] assumptions discards transverse shear and through-the-thickness deformation. The displacement model related to the CLT can be written in the following forms:

$$u_\tau(x,y,z;t) = u_{0\tau}(x,y;t) - z\frac{\partial u_{0z}(x,y;t)}{\partial \tau}, \quad \tau = x,y \tag{1}$$

$$u_z(x,y,z;t) = u_{0z}(x,y;t) \tag{2}$$

which state that the section remains plane and orthogonal to the plate reference surface Ω. t denotes time; u_0 denotes the displacement value in correspondence to the reference surface Ω. Figure 2 shows the displacement field related to the CLT. Transverse shear stresses are discarded in the CLT analysis. These could be obtained a posteriori by integrating the 3D indefinite equilibrium equations.

2.2 The First Order Shear Deformation Theory. Transverse shear deformation can be introduced into CLT theories according to the following kinematic assumptions, known as the Reissner–Mindlin [16,17] theory:

$$u_\tau(x,y,z;t) = u_{0\tau}(x,y;t) + zu_{1\tau}(x,y;t), \quad \tau = x,y \tag{3}$$

$$u_z(x,y,z;t) = u_{0z}(x,y;t) \tag{4}$$

which is also denoted as the FSDT. $u_{1\tau}$ denotes transverse rotations. Figure 3 shows the displacement field related to the FSDT. The transverse shear stresses show an "a priori" constant piecewise distribution. As in the CLT case, better results can be obtained through an "a posteriori" integration of the 3D indefinite equilibrium equations.

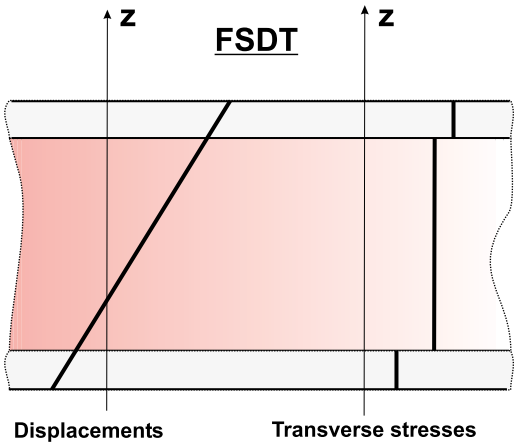

Fig. 3 Displacements and transverse stresses in the case of first order shear deformation theory

3 The Higher Order Theories

3.1 HOTs Including Transverse Normal Strain. Refinements of CLT and FSDT analyses can be introduced by including higher order terms in the kinematic assumptions made for the displacements field,

$$u_\tau(x,y,z;t) = u_{0\tau}(x,y;t) + z^r u_{r\tau}(x,y;t), \quad \tau = x,y,z, \quad r = 1,N \tag{5}$$

The summing convention for repeated indices has been adopted; N is the order of expansion, which is taken as a free parameter. In this paper, the values from $N=1$ to $N=4$ are considered in the numerical investigation. According to the unified formulation, the related theories are denoted as ED1–ED4. The letter E denotes that the kinematics is preserved for all the plate layers, as in the so-called ESL. D denotes that only displacement unknowns are used, and the last digit denotes the order of expansion N in z. Typical displacements and transverse stress evaluations are reported in Fig. 4 for ED2.

3.2 HOTs Discarding Transverse Normal Strain. In the case in here transverse normal strains are discarded; the following condition should be considered for the transverse displacement:

$$u_z(x,y,z;t) = u_{0z}(x,y;t) \tag{6}$$

Related theories are denoted by adding the suffix d to the acronyms ($ED1_d, \ldots, ED4_d$).

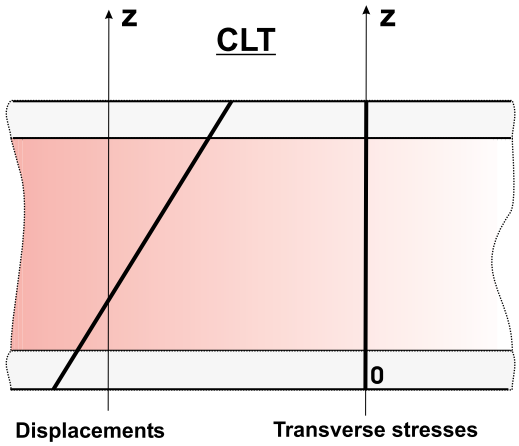

Fig. 2 Displacements and transverse stresses in the case of classical lamination theory

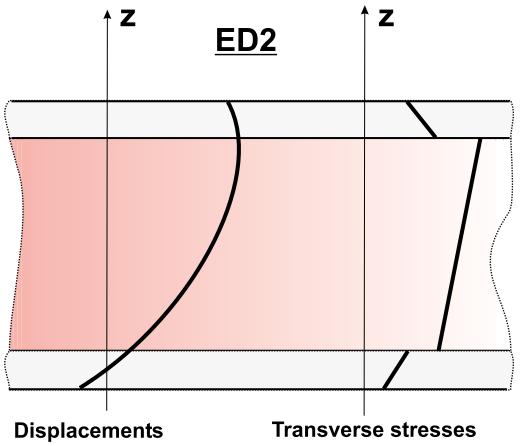

Fig. 4 Displacements and transverse stresses in the case of ED2

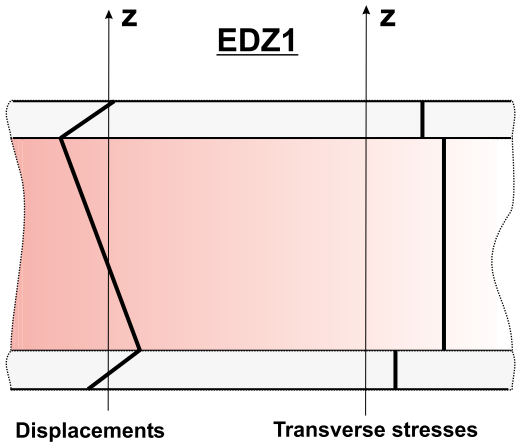

Fig. 5 Displacements and transverse stresses in the case of EDZ1

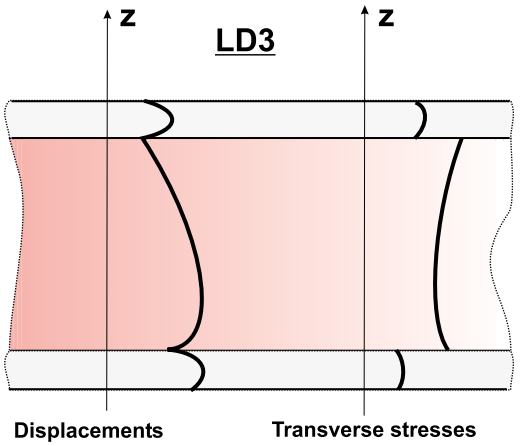

Fig. 6 Displacements and transverse stresses in the case of LD3

3.3 HOTs Including Zigzag Effects. ED*N* models are not able to describe zigzag effects in the case of sandwiches and laminates. The discontinuity of the first derivative, in correspondence to the layer interfaces, can be introduced by employing Murakami's zigzag function (MZZF), which was proposed in the framework of RMVT applications [82]. The nondimensional layer coordinate $\zeta_k=(2z_k)/h_k$ is also introduced (h_k is the thickness of the kth layer and z_k is the layer thickness coordinate). Murakami's zigzag function $M(z)$ is defined according to the following formula:

$$M(z) = (-1)^k \zeta_k \tag{7}$$

$M(z)$ has the following properties: It is a piecewise linear function of the layer coordinates z_k; $M(z)$ has unit amplitude for all the layers; the slope $M'(z)=dM/dz$ assumes an opposite sign between two adjacent layers (its amplitude is layer thickness independent). The displacement that includes MZZF is written in the form

$$u_\tau(x,y,z;t) = u(x,y;t)_{0\tau} + z^r u(x,y;t)_{r\tau} + (-1)^k \zeta_k u(x,y;t)_{Z\tau},$$

$$\tau = x,y,z, \quad r = 1,2,\ldots,N-1 \tag{8}$$

The subscript Z refers to the introduced zigzag term. Higher order distributions in the z-direction are introduced by the r-polynomials.

Modifications of ED*N* to include MZZF are herein denoted as EDZ*N* analyses. Figure 5 shows the displacement and transverse stress field related to EDZ1 kinematics. It is anticipated that the use of MZZF will turn out to be very beneficial for the modeling of sandwich structures.

4 The Layerwise Theories

A multilayered plate can be analyzed using kinematic assumptions that are independent in each layer. According to Ref. [24], these approaches have herein been called layerwise theories. A layerwise description requires that independent displacement variables be assumed in each k-layer. The Taylor thickness expansion used for the ESLM cases in the previous sections is not convenient for a layerwise description. Interlaminar continuity for displacements can be more conveniently imposed by employing interface values as unknown variables. Therefore, a layerwise description is written according to the following expansion:

$$u_\tau^k = F_t u_\tau^k + F_b u_{\tau b}^k + F_r u_{\tau r}^k, \quad \tau = x,y,z,$$

$$r = 2,3,\ldots,N, \quad k = 1,2,\ldots,N_l \tag{9}$$

The subscripts t and b denote values related to the top and bottom layer surfaces, respectively. The thickness functions $F_\tau(\zeta_k)$ have been defined by

$$F_t = \frac{P_0 + P_1}{2}, \quad F_b = \frac{P_0 - P_1}{2}, \quad F_r = P_r - P_{r-2}, \quad r = 2,3,\ldots,N \tag{10}$$

in which $P_j=P_j(\zeta_k)$ is the Legendre polynomial of the j-order defined in the ζ_k-domain: $-1\leqslant\zeta_k\leqslant 1$. A fourth order case is used in the numerical investigations; the related polynomials are

$$P_0 = 1, \quad P_1 = \zeta_k, \quad P_2 = (3\zeta_k^2 - 1)/2, \quad P_3 = \frac{5\zeta_k^3}{2} - \frac{3\zeta_k}{2},$$

$$P_4 = \frac{35\zeta_k^4}{8} - \frac{15\zeta_k^2}{4} + \frac{3}{8}$$

The chosen functions have the following properties:

$$\zeta_k = \begin{cases} 1: & F_t = 1, \quad F_b = 0, \quad F_r = 0 \\ -1: & F_t = 0, \quad F_b = 1, \quad F_r = 0 \end{cases} \tag{11}$$

The top and bottom values have been used as unknown variables. The interlaminar compatibility of displacement can therefore be easily linked,

$$u_\tau^k = u_{\tau b}^{(k+1)}, \quad k = 1, N_l - 1 \tag{12}$$

According to the unified formulation, the related theories are denoted as LD1–LD4, where the letter L means layerwise approach. A typical evaluation of displacements and transverse stresses is reported in Fig. 6 for the case of LD3.

5 The Mixed Theories Based on Reissner's Mixed Variational Theorem

It is a well known fact that the above described kinematics [80] are not able to furnish a priori interlaminar continuous transverse shear or normal stresses at the interface between two adjacent layers when applied to multilayered structures. Reissner's mixed variational theorem [56,48] offers the possibility of a priori fulfilling such an interlaminar continuity. Both displacements and transverse shear and normal stresses can, in fact, be assumed in the RMVT framework.

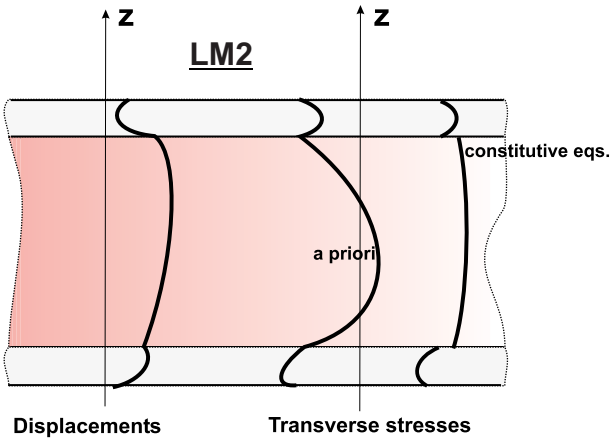

Fig. 7 Displacements and transverse stresses in the case of LM2

5.1 The Layerwise Mixed Theories. In the layerwise case, the displacement model in Eq. (9) is also used for the transverse stress variables,

$$\sigma^k_{\tau z} = F_t \sigma^k_{\tau z_t} + F_b \sigma^k_{\tau z_b} + F_r \sigma^k_{\tau z_r}, \quad \tau = x,y,z,$$

$$r = 2,3,\ldots,N, \quad k = 1,2,\ldots,N_l \tag{13}$$

The interlaminar transverse shear and normal stress continuity can therefore be easily linked,

$$\sigma^k_{\tau z_t} = \sigma^{(k+1)}_{\tau z_b}, \quad \tau = x,y,z, \quad k = 1,N_l - 1 \tag{14}$$

These are denoted as LM1–LM4, where M means mixed models. The displacements and transverse stresses are reported in Fig. 7 for the case of LM2.

5.2 The Equivalent Single Layer Mixed Theories. Mixed theories with equivalent single layer descriptions can be used by referring to the displacement model in Eq. (5) and the layerwise stress assumption in Eq. (13). These are referred to as EM1–EM4. A typical evaluation of EM2 is illustrated in Fig. 8. If the displacement model is that of Eq. (8), the models are EMZ1–EMZ3.

5.3 Unified Formulation. The previous models have been coded according to the unified formulation. Details can be found in the first author's previous works [80]. All ESL theories with constant or linear transverse displacement u_z (e.g. CLT, FSDT, ED1, EDZ1, EMZ1, EM1) make use of plane stress conditions for the constitutive equations to contrast the thickness locking (TL) phenomena illustrated in Ref. [81].

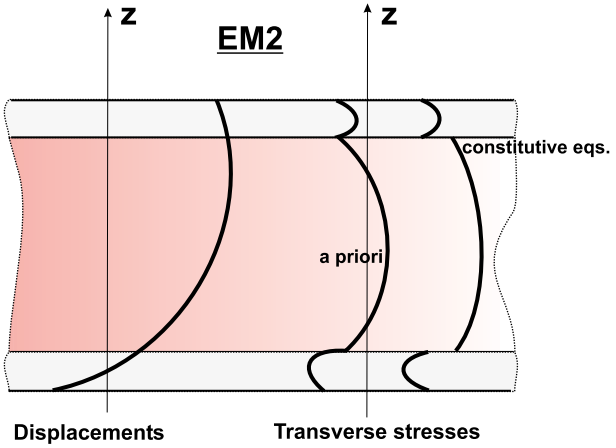

Fig. 8 Displacements and transverse stresses in the case of EM2

Table 1 Benchmark 1. Elastic and geometrical properties of a sandwich plate with a core in Nomex.

Properties	Layer 1–3 (Al 2024)
E (GPa)	73
ν	0.34
G (GPa)	27.239
ρ (kg/m^3)	2800
$h_1 = h_3$ (m)	0.1
a/b	4, 10, 100, 1000
	Layer 2 (Nomex)
$E_L = E_T$ (MPa)	0.01
E_z (MPa)	75.85
ν	0.01
G (MPa)	22.5
ρ (kg/m^3)	32
h_2 (m)	0.8
a/b	4, 10, 100, 1000

6 Benchmark Description

Simply supported sandwich plates made of orthotropic materials have been dealt with the bisinusoidal distribution of transverse pressure applied to the top plate surface,

$$p_z(x,y) = \bar{p}_z \sin\left(\frac{m\pi x}{a}\right)\sin\left(\frac{n\pi y}{b}\right) \tag{15}$$

where $\bar{p}_z$ is the applied load amplitude, m and n are the wave numbers in the two in-plane plate directions, and a and b are the corresponding plate dimensions. Attention has been restricted to the cases where $m=1$ and $n=1$.

In the case of free vibration problems, the results are mostly restricted to the first fundamental bending circular frequency parameter $\bar{\omega} = \omega\sqrt{a^4(\rho)_{\text{skin}}/(E_T)_{\text{skin}}h^2}$, where a and h are the dimensions and the thickness of the plate, respectively; ρ and E_T are the mass density and the transverse Young's modulus of the skin. In order to highlight both the advantages and limitations of the considered kinematic models, various sandwich panels have been analyzed. Numerical investigations and comparisons of various theories have been conducted by varying the following two parameters:

- LTR (a/h): length-to-thickness ratio; this is a geometrical parameter.
- FCSR (E_f/E_c): face-to-core-stiffness ratio; this is a mechanical parameter. E_f and E_c represent Young's module of the face and core, respectively.

Aluminum alloys and carbon fiber reinforced plastic (CFRP) materials have been used for the skins while Nomex has been considered for the core. Stiffer and more deformable cores have been obtained by multiplying the Nomex mechanical properties by various factors. The following three benchmarks were first analyzed.

Benchmark 1 (B1): Metallic faces and Nomex core. All the data concerning the considered panels are given in Table 1. Young's modulus parameter ratios between the skins and core are

$$\text{FCSR}_L = E_f/E_{cL} = 7.3E6, \quad \text{FCSR}_z = E_f/E_{cz} = 962.4$$

where subscript L stands for fiber and z for the thickness direction, respectively.

Benchmark 2 (B2): Metallic faces and a softer core. The

Table 2 Benchmark 2. Elastic and geometrical properties of a sandwich plate with reduced core stiffness.

Properties	Layers 1–3 (Al 2024)
E (GPa)	73
ν	0.34
G (GPa)	27.239
ρ (kg/m^3)	2800
$h_1=h_3$ (m)	0.1
$a=b$	4, 10, 100, 1000
	Layer 2 (Nomex: modulus divided by 100)
$E_L=E_T$ (MPa)	0.0001
E_z (MPa)	0.7585
ν	0.01
G (MPa)	0.225
ρ (kg/m^3)	0.32
h_2 (m)	0.8
$a=b$	4, 10, 100, 1000

Nomex core properties were reduced by a factor of 100. The authors are aware that this way of reducing properties is not physically sound, but it appears reasonable for the aim of this work. All the data concerning the considered panels are given in Table 2. Young's moduli parameter ratios between the skins and faces hold,

$$\mathrm{FCSR}_L = E_f/E_{cL} = 7.3E8, \quad \mathrm{FCSR}_z = E_f/E_{cz} = 9.624E4$$

Benchmark 3 (B3): Composite faces and Nomex core. The skin consists of two layers of cross-ply laminated CFRP. The core is the same as that used in Benchmark 1. For the readers' convenience, the data have been repeated in each table. All the data of the considered panels are given in Table 3. Young's moduli parameter ratios between the skins and faces are

$$\mathrm{FCSR}_L = E_{fL}/E_{cL} = 5.0E6, \quad \mathrm{FCSR}_z = E_{fz}/E_{cz} = 131.84$$

7 Results and Discussion

Navier-type closed form solutions of simply supported isotropic and orthotropic square plates are discussed. The readers can refer to previous works [48,76] to find details of the implemented unified formulation and solution procedure.

Table 3 Benchmark 3. Elastic and geometrical properties of a sandwich plate with composite skins.

Properties	Layers 1 and 2 and 3 and 4 (cross-ply CFRP)
E_L (GPa)	50
$E_T=E_z$ (GPa)	10
ν	0.25
G (GPa)	5
ρ (kg/m^3)	1600
$h_1=h_2=h_4=h_5$ (m)	0.05
$a=b$	4, 10, 100, 1000
ϑ: orientation (deg)	0/90 and 90/0
	Layers 3 (Nomex), as in Table 1
$E_L=E_T$ (MPa)	0.01
E_z (MPa)	75.85
ν	0.01
G (MPa)	22.5
ρ (kg/m^3)	32
h_3 (m)	0.8
$a=b$	4, 10, 100, 1000

Table 4 Elastic and geometrical properties of a sandwich plate with isotropic core and skins, used for the comparison with the 3D analysis

Properties	Layers 1–3
E (GPa)	50
ν	0.25
G (GPa)	20
ρ (kg/m^3)	1
$h_1=h_3$ (m)	0.1
$b=3a$	3, 300
	Layer 2
E (GPa)	1
ν	0.25
G (GPa)	0.4
ρ (kg/m^3)	1
h_2 (m)	0.8
$b=3a$	3, 300

A large numerical investigation has been conducted to compare the various theories that were illustrated in the previous section. The results are discussed in the following sections, which give a rather exhaustive overview of the performance of classical and advanced theories as tools to analyze sandwich plates.

7.1 Preliminary Assessment Versus 3D. A preliminary assessment of the used UF was made through a comparison with the 3D analysis by Demasi [11]. Isotropic materials were considered for both the core and skins. Young's moduli ratio is

$$\mathrm{FCSR} = E_f/E_c = 50$$

All the data concerning this panel are given in Table 4. The results are shown in Table 5. The layerwise mixed results are considered. It has been concluded that the LM4 analysis can be used as a quasi-3D solution for those cases in which complete 3D results are not available. This could make it possible to assess various theories of all the proposed benchmarks. $a/h=1$ was chosen to highlight the capability of the LM4 analysis to trace a complete 3D response.

7.2 The Classical and First Order Shear Deformation Plate Theory. Table 6 compares CLT and FSDT analyses with 3D solutions for Benchmarks 1, 2, and 3. The quoted 3D solutions correspond to the LM4 analyses. Maximum transverse displacements in correspondence to the middle surface are given for various values of the thickness ratio (LTR); the percentage error is placed in brackets. CLT and FSDT are never reliable for thick

Table 5 Preliminary assessment. Comparison between LM4 and 3D solution by Demasi [11]. $E_f/E_c=50$. $\bar{u}_x = U_x(E_c/\bar{p}_z h(a/h)^3)$, $\bar{u}_y = U_y(E_c/\bar{p}_z h(a/h)^3)$, and $\bar{u}_z = U_z(100E_c/\bar{p}_z h(a/h)^4)$.

	$a/h=1$		$a/h=100$	
	3D	LM4	3D	LM4
$\bar{u}_x(-h/2)$	0.01397	0.01397	0.00590	0.00590
$\bar{u}_x(0)$	0.05864	0.05864	0.0000	0.0000
$\bar{u}_x(h/2)$	−0.05928	−0.05928	−0.00590	−0.00590
$\bar{u}_y(-h/2)$	0.00466	0.00466	0.00197	0.00197
$\bar{u}_y(0)$	0.01955	0.01955	0.0000	0.0000
$\bar{u}_y(h/2)$	−0.01976	−0.01976	−0.00197	−0.00197
$\bar{u}_z(-h/2)$	7.1045	7.1047	0.37774	0.37774
$\bar{u}_z(0)$	15.054	15.050	0.37776	0.37776
$\bar{u}_z(h/2)$	36.119	36.118	0.37774	0.37774

Table 6 Comparison between 3D solutions versus classical ones. Transverse displacement evaluations $\bar{u}_z = U_z(100(E_T)_{skin}h^3/\bar{p}_z a^4)$ at the midsurface. Static analysis.

a/h	4	Error	10	Error	100	Error	1000	Error
				Benchmark 1				
3D	590.54	%	149.70	%	7.1881	%	5.5980	%
CLT	5.5799	(99.0)	5.5799	(96.3)	5.5799	(22.4)	5.5799	(0.32)
FSDT	9.8087	(98.3)	6.2565	(95.8)	5.5867	(22.3)	5.5800	(0.32)
				Benchmark 2				
3D	1370.6	%	1260.3	%	149.51	%	7.1901%	
CLT	5.5815	(99.6)	5.5815	(99.6)	5.5815	(96.3)	5.5815	(22.4)
FSDT	9.8241	(99.3)	6.2603	(99.5)	5.5883	(96.3)	5.5815	(22.4)
				Benchmark 3				
3D	124.69	%	24.545	%	3.1589	%	2.9360	%
CLT	2.9382	(97.6)	2.9382	(88.0)	2.9382	(6.99)	2.9382	(0.07)
FSDT	6.0535	(95.1)	3.4371	(86.0)	2.9432	(6.83)	2.9383	(0.08)

$(a/h=4)$ or moderately thick $(a/h=10)$ sandwich plates. Their application to thin $(a/h=100)$ and very thin $(a/h=1000)$ sandwich plates appears to be very much subordinate to the FCSR. Large errors $(\approx 22\%)$ are, in fact, obtained in the B2 case even though very thin plates are considered.

Significant stress evaluations are given in Tables 7 and 8. In-plane normal stresses and transverse shear stresses are compared. The latter ones were computed in two different ways: By integrating 3D equilibrium equations and by using constitutive equations. The accuracy of the stress evaluations appears higher than those exhibited by transverse displacements. It has been confirmed that transverse stresses from 3D equilibrium equations are more accurate than those corresponding to Hooke's constitutive law. However, the errors are still not acceptable.

The previous comments were confirmed using the free vibration evaluation analysis reported in Table 9. Higher vibration modes are considered in Table 10, and these show larger errors with respect to $m=1$ and $n=1$ cases. It can be concluded that CLT and FSDT are not suitable for application to sandwich plates even when very thin panels are considered.

Distributions of in-plane and transverse stress variables in the thickness direction are given in Figs. 9 and 10. In-plane and transverse shear stress components have been plotted, respectively. It has been confirmed that the accuracy of classical plate theories is very much subordinate to the value of the thickness coordinate z. The results have been restricted to B1 sandwich plates.

7.3 The Higher Order Theory and Transverse Normal Strain Effects. HOTs with linear up to fourth order expansion in the sandwich thickness direction are compared in Table 11 for the B1 and B2 sandwich plates. Significant stress evaluations are given in Table 12. Improvements should occur with respect to classical theories; the quoted error, however, still renders HOT unsuitable for sandwich plates. This has been confirmed for very thin plates and B2 cases. It appears clear that the error due to high values of the FCSR parameter plays a predominant role. The effect of transverse normal strain has been evaluated in Table 13. It should be noticed that the error can double if through-the-thickness deformations are neglected in the analysis.

7.4 The Higher Order Theory With Zigzag Kinematics. The advantages of using Murakami's zigzag functions are evaluated in Table 14. The given results clearly show the convenience of using MZZF in the modeling of sandwich structures. MZZF, in fact, introduces very significant benefits with respect to HOT, which make use of the same number of degrees of freedom (see Fig. 5). The error is greatly reduced with respect to the ED1–ED4 theories discussed in the previous section. The same conclusions can be drawn for the stress evaluations given in Table 15 and for the vibration response in Table 16.

In Tables 14–16, EDZ1 uses plane stress conditions to avoid the thickness locking (TL) phenomena, and the considered problem shows that EDZ1 leads to better results than EDZ2 and EDZ3. In general, the use of plane stress conditions improves the EDZ1

Table 7 Benchmark 1. Sandwich plate with a core in Nomex. Static analysis. In-plane σ_{xx} and transverse shear σ_{xz} stresses. Comparison between 3D solutions versus classical ones.

a/h	4	Error	100	Error
		$\sigma_{xx}(z=h/2)$		
3D	67.958	%	4288.0	%
CLT	6.6753	(90.2)	4172.1	(2.70)
FSDT	6.6753	(90.2)	4172.1	(2.70)
		$\sigma_{xz}(z=0)$ from 3D equations		
3D	0.4053	%	17.594	%
CLT	0.7046	(73.8)	17.615	(0.12)
FSDT	0.7046	(73.8)	17.615	(0.12)
		$\sigma_{xz}(z=0)$ from constitutive equations		
3D	0.4053	%	17.594	%
CLT	—	—	—	—
FSDT	0.0026	(99.3)	0.0655	(99.6)

Table 8 Benchmark 2. Sandwich plate with reduced core stiffness. Static analysis. In-plane σ_{xx} and transverse shear σ_{xz} stresses. Comparison between 3D solutions versus classical ones.

a/h	4	Error	100	Error
		$\sigma_{xx}(z=h/2)$		
3D	408.06	%	14535	%
CLT	6.6772	(98.4)	4173.2	(71.3)
FSDT	6.6772	(98.4)	4173.2	(71.3)
		$\sigma_{xz}(z=0)$ from 3D equations		
3D	0.0094	%	15.743	%
CLT	0.7045	(>100)	17.611	(11.9)
FSDT	0.7045	(>100)	17.611	(11.9)
		$\sigma_{xz}(z=0)$ from constitutive equations		
3D	0.0094	%	15.743	%
CLT	—	—	—	—
FSDT	0.00003	(99.7)	0.0007	(100)

Table 9 Comparison between 3D solutions versus classical ones. Free vibration problem. Fundamental frequency: $\bar{\omega}=\omega\sqrt{a^4(\rho)_{skin}/(E_T)_{skin}h^2}$. $m,n=1$.

a/h	4	Error	10	Error	100	Error	1000	Error
				Benchmark 1				
3D	0.9063	%	1.7891	%	8.1549	%	9.2419	%
CLT	8.3037	(>100)	9.0822	(>100)	9.2551	(13.5)	9.2569	(0.16)
FSDT	6.7086	(>100)	8.6096	(>100)	9.2495	(13.4)	9.2568	(0.16)
				Benchmark 2				
3D	0.4911	%	0.6305	%	1.8283	%	8.3371	%
CLT	8.4610	(>100)	9.2783	(>100)	9.4607	(>100)	9.4626	(13.5)
FSDT	6.8448	(>100)	8.7952	(>100)	9.4550	(>100)	9.4625	(13.5)
				Benchmark 3				
3D	1.9398	%	4.3461	%	12.104	%	12.557	%
CLT	11.285	(>100)	12.321	(>100)	12.550	(3.68)	12.552	(0.04)
FSDT	8.4963	(>100)	11.447	(>100)	12.539	(3.59)	12.552	(0.04)

Table 10 Benchmark 1. Sandwich plate with a core in Nomex. Free vibration problem. Fundamental frequency related to $m=n=2$: $\bar{\omega}=\omega\sqrt{a^4(\rho)_{skin}/(E_T)_{skin}h^2}$. Comparison between 3D solutions versus classical ones.

a/h	4	Error	10	Error	100	Error	1000	Error
3D	2.4938	%	4.1634	%	25.256	%	36.816	%
CLT	21.131	(>100)	34.448	(>100)	36.999	(46.5)	37.027	(0.57)
FSDT	17.812	(>100)	29.336	(>100)	36.910	(46.1)	37.026	(0.57)

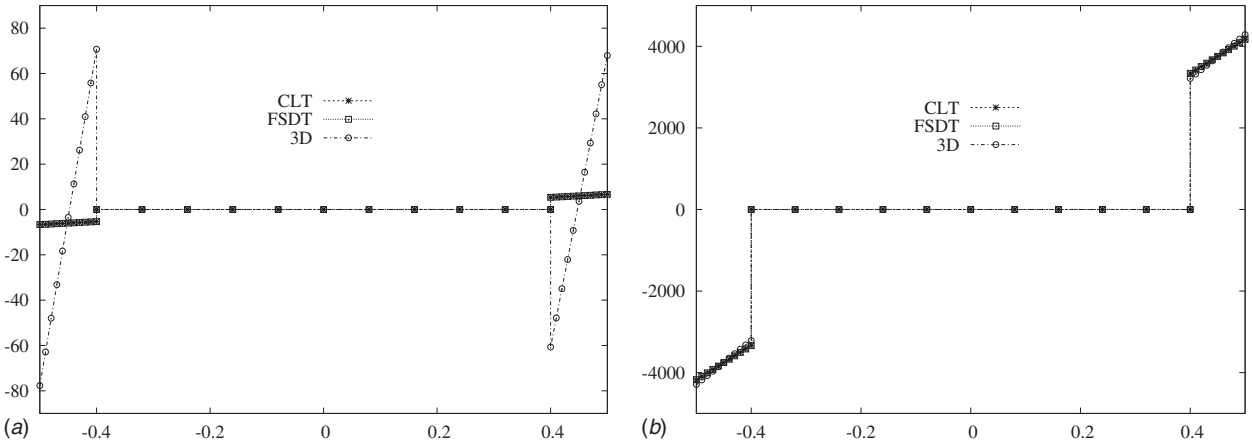

Fig. 9 Benchmark 1. Sandwich plate with a core in Nomex. Static analysis. σ_{xx} versus z. Comparison between 3D solutions and classical theories. $a/h=4$ on the left. $a/h=100$ on the right.

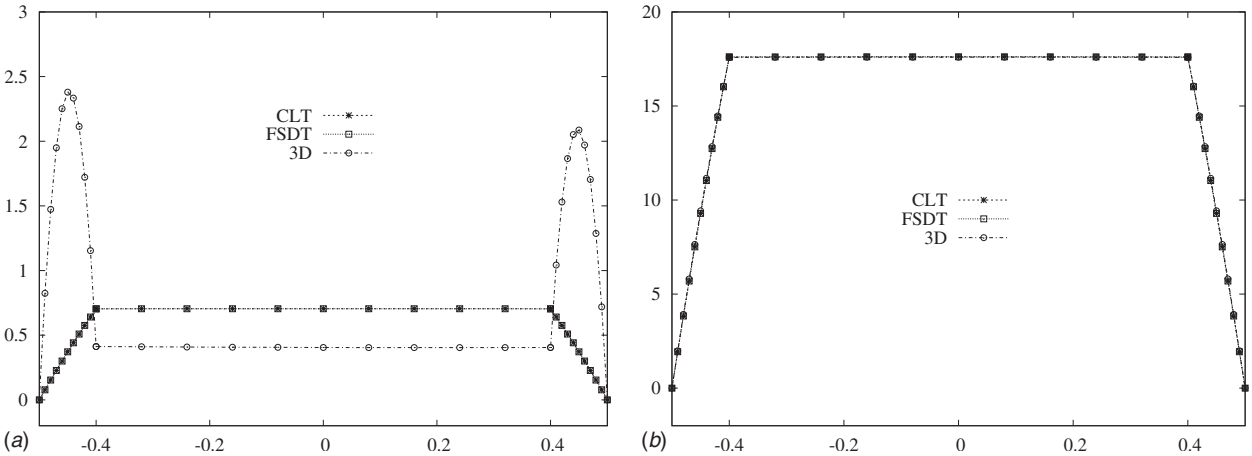

Fig. 10 Benchmark 1. Sandwich plate with a core in Nomex. Static analysis. σ_{xz} versus z. Comparison between 3D solutions and classical theories. $a/h=4$ on the left. $a/h=100$ on the right.

Table 11 Comparison between 3D solutions versus HOT theories. Transverse displacement evaluations $\bar{u}_z = U_z 100(E_T)_{skin}/h^3\bar{p}_z a^4$ at mid surface. Static analysis.

a/h	4	Error	10	Error	100	Error	1000	Error
				Benchmark 1				
3D	590.54	%	149.70	%	7.1881	%	5.5980	%
ED1	9.8087	(98.3)	6.2565	(95.8)	5.5867	(22.3)	5.5800	(0.32)
ED2	10.067	(98.3)	6.3027	(95.8)	5.5897	(22.2)	5.5825	(0.28)
ED3	100.85	(82.9)	22.059	(85.3)	5.7498	(20.0)	5.5841	(0.25)
ED4	101.72	(82.8)	22.086	(85.2)	5.7498	(20.0)	5.5842	(0.25)
				Benchmark 2				
3D	1370.6	%	1260.3	%	149.51	%	7.1901	%
ED1	9.8241	(99.3)	6.2603	(99.5)	5.5883	(96.3)	5.5815	(22.4)
ED2	10.081	(99.3)	6.3042	(99.5)	5.5887	(96.3)	5.5816	(22.4)
ED3	111.42	(91.9)	24.045	(98.1)	5.7693	(96.1)	5.5834	(22.3)
ED4	112.53	(91.8)	24.083	(98.1)	5.7693	(96.1)	5.5834	(22.3)

Table 12 Comparison between 3D solutions versus HOT theories. Static analysis. Transverse shear σ_{xz} stress at the midsurface obtained from 3D equilibrium equations.

a/h	4	Error	100	Error
		Benchmark 1		
3D	0.4053	%	17.594	%
ED1	0.7046	(73.8)	17.615	(0.12)
ED2	0.7046	(73.8)	17.615	(0.12)
ED3	0.6393	(57.7)	17.612	(0.10)
ED4	0.6559	(61.8)	17.611	(0.10)
		Benchmark 2		
3D	0.0094	%	15.743	%
ED1	0.70446	(>100)	17.611	(11.9)
ED2	0.70446	(>100)	17.611	(11.9)
ED3	0.63279	(>100)	17.608	(11.8)
ED4	0.65018	(>100)	17.609	(11.8)

Table 13 Benchmark 1. Comparison between 3D solutions versus HOT theories. ϵ_{zz} effect. $\bar{u}_z = U_z(100(E_T)_{skin}h^3/\bar{p}_z a^4)$ at the midsurface. Static analysis.

a/h	4	Error	100	Error
3D	590.54	%	7.1881	%
ED1	9.8087	(98.3)	5.5867	(22.3)
ED4	101.72	(82.8)	5.7498	(20.0)
$ED1_d$	9.8087	(98.3)	5.5867	(22.3)
$ED4_d$	99.550	(83.1)	4.2670	(40.6)

Table 15 Comparison between 3D solutions versus HOT theories with MZZF. Static analysis. Transverse shear σ_{xz} stress at the midsurface obtained from 3D equilibrium equations.

a/h	4	Error	100	Error
		Benchmark 1		
3D	0.4053	%	17.594	%
EDZ1	0.4034	(0.47)	17.594	(0.00)
EDZ2	0.3499	(13.7)	17.586	(0.04)
EDZ3	0.3499	(13.7)	17.586	(0.04)
		Benchmark 2		
3D	0.0094	%	15.743	%
EDZ1	0.0093	(1.06)	15.743	(0.00)
EDZ2	0.0069	(26.6)	15.161	(3.70)
EDZ3	0.0069	(26.6)	15.161	(3.70)

model with respect to the 3D solution and TL phenomena but not with respect to EDZ2 and EDZ3 (see Ref. [81]): in the present case, the core is very soft, and the plane stress conditions greatly reduce the stiffness, leading to better results.

Distributions of the transverse stress variables in the thickness direction are given in Fig. 11. Results related to the use of MZZF with cubic expansion (EDZ3) are compared to 3D and classical theory results. The advantages of using MZZF are clearly confirmed.

7.5 Use of Layerwise Kinematics. The results related to the use of layerwise kinematic are given in Tables 17–19. These clearly show that layerwise analyses are the only ones that are able to deal with the modeling of sandwich structures with an

Table 14 Comparison between 3D solutions versus HOT theories with MZZF. $\bar{u}_z = U_z(100(E_T)_{skin}h^3/\bar{p}_z a^4)$ at the midsurface. Static analysis.

a/h	4	Error	10	Error	100	Error	1000	Error
				Benchmark 1				
3D	590.54	%	149.70	%	7.1881	%	5.5980	%
EDZ1	58405	(1.10)	149.53	(0.11)	7.1883	(0.00)	5.5960	(0.03)
EDZ2	507.40	(14.1)	144.20	(3.67)	7.1899	(0.02)	5.5986	(0.01)
EDZ3	507.40	(14.1)	144.20	(3.67)	7.1899	(0.02)	5.5986	(0.01)
				Benchmark 2				
3D	1370.6	%	1260.3	%	149.51	%	7.1901	%
EDZ1	1348.0	(1.65)	1257.1	(0.25)	149.50	(0.01)	7.1896	(0.01)
EDZ2	996.59	(27.3)	944.52	(25.0)	144.19	(3.56)	7.1890	(0.01)
EDZ3	996.59	(27.3)	944.52	(25.0)	144.19	(3.56)	7.1890	(0.01)

Table 16 Comparison between 3D solutions vs HOT theories and HOT theories with MZZF. Free vibrations problem. Fundamental frequency: $\bar{\omega}=\omega\sqrt{a^4(\rho)_{skin}/(E_T)_{skin}h^2}$. $m,n=1$.

a/h	4	Error	10	Error	100	Error	1000	Error
				Benchmark 1				
3D	0.9063	%	1.7891	%	8.1549	%	9.2419	%
ED1	6.7086	(>100)	8.6096	(>100)	9.2495	(13.4)	9.2568	(0.16)
ED4	2.1515	(>100)	4.6467	(>100)	9.1177	(11.8)	9.2533	(0.12)
EDZ1	0.9043	(0.22)	1.7880	(0.06)	8.1548	(0.00)	9.2435	(0.02)
EDZ3	0.9704	(7.07)	1.8210	(1.78)	8.1541	(0.01)	9.2414	(0.00)
				Benchmark 2				
3D	0.4911	%	0.6305	%	1.8283	%	8.3371	%
ED1	6.8448	(>100)	8.7952	(>100)	9.4550	(>100)	9.4625	(13.5)
ED4	2.0916	(>100)	4.5498	(>100)	9.3059	(>100)	9.4610	(13.5)
EDZ1	0.6086	(23.9)	0.6305	(0.00)	1.8283	(0.00)	8.3374	(0.00)
EDZ3	0.7079	(44.1)	0.7274	(15.4)	1.8617	(1.83)	8.3378	(0.01)

accuracy that is independent of both the geometric properties (LTR) and the mechanical properties of the faces and core (FCSR). This has been confirmed for both bending and vibration responses.

Distributions of transverse stress variables in the thickness direction are given in Fig. 12. LD4 results are compared to the significant ESLM analysis. It appears clear that the accuracy of LW analyses leads to 3D descriptions of stress fields in both the core and faces of sandwich structures. EDZ*N* gives good local results, but Fig. 12 clearly shows the superiority of LW analyses to evaluate transverse shear stresses in the two skins.

7.6 Mixed Theories. The results for mixed theories based on RMVT are given in Tables 20–23. ESL results are given in Table 20. Improvements have been found with respect to displacement formulated theories. However, the main limitations of the ESL analysis used to analyze soft-core sandwich structures are confirmed. Layerwise mixed results are given in another three tables,

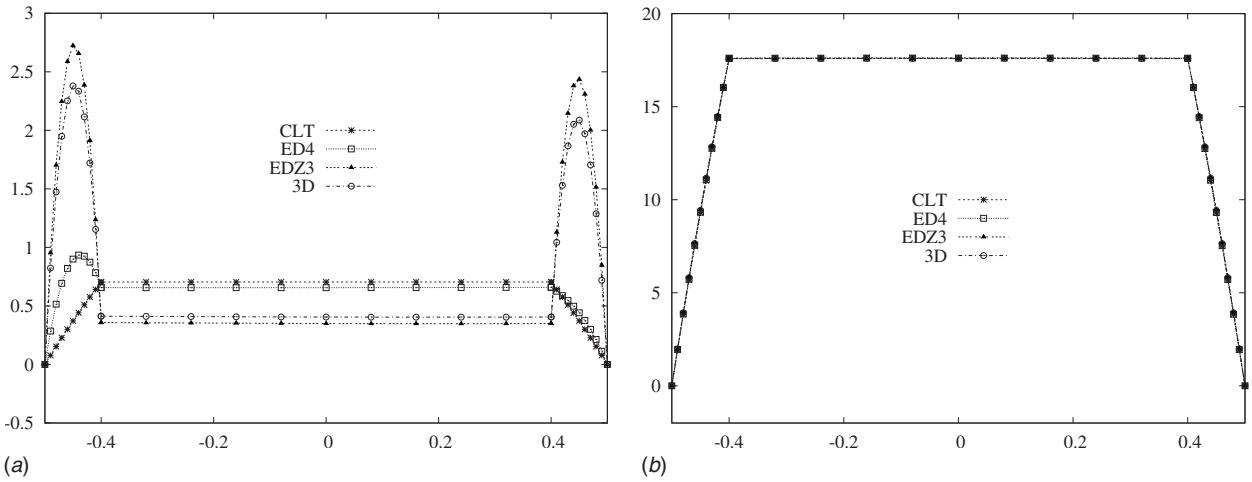

Fig. 11 Benchmark 1. Sandwich plate with a core in Nomex. Static analysis. σ_{xz} versus z. Comparison between 3D solutions, HOT theories, and HOT theories with MZZF. $a/h=4$ on the left. $a/h=100$ on the right.

Table 17 Comparison between 3D solutions versus layerwise models. Transverse displacement evaluations $\bar{u}_z=U_z(100(E_T)_{skin}h^3/\bar{p}_z a^4)$ at the midsurface. Static analysis.

a/h	4	Error	10	Error	100	Error
			Benchmark 1			
3D	590.54	%	149.70	%	7.1881	%
LD1	506.22	(14.3)	143.82	(3.93)	7.1744	(0.19)
LD2	590.45	(0.01)	149.70	(0.00)	7.1881	(0.00)
LD3	590.54	(0.00)	149.70	(0.00)	7.1881	(0.00)
LD4	590.54	(0.00)	149.70	(0.00)	7.1881	(0.00)
			Benchmark 2			
3D	1370.6	%	1260.3	%	149.51	%
LD1	994.85	(27.4)	943.01	(25.2)	143.80	(3.82)
LD2	1370.1	(0.04)	1260.2	(0.01)	149.51	(0.00)
LD3	1370.6	(0.00)	1260.3	(0.00)	149.51	(0.00)
LD4	1370.6	(0.00)	1260.3	(0.00)	149.51	(0.00)

Table 18 Comparison between 3D solutions versus layerwise models. Static analysis. Transverse shear σ_{xz} stress at the midsurface.

a/h	4	Error	100	Error
		Benchmark 1		
3D	0.4053	%	17.594	%
LD1	0.3496	(13.7)	17.560	(0.19)
LD2	0.4052	(0.02)	17.594	(0.00)
LD3	0.4053	(0.00)	17.594	(0.00)
LD4	0.4053	(0.00)	17.594	(0.00)
		Benchmark 2		
3D	0.0094	%	15.743	%
LD1	0.0069	(26.6)	15.142	(3.82)
LD2	0.0094	(0.00)	15.743	(0.00)
LD3	0.0094	(0.00)	15.743	(0.00)
LD4	0.0094	(0.00)	15.743	(0.00)

which deal with displacement, stress, and vibration evaluations, respectively. The convenience of referring to a layerwise analysis has been confirmed for the mixed cases. Better results have been obtained with respect to the related formulations with only displacement variables.

7.7 ESLM Versus LWM in the Soft-Core Cases. The previous analysis has highlighted the difficulties involved in the use

Table 19 Comparison between 3D solutions versus layerwise models. Free vibration problem. Fundamental frequency: $\bar{\omega} = \omega\sqrt{a^4(\rho)_{skin}/(E_T)_{skin}h^2}$. $m,n=1$.

a/h	4	Error	10	Error	100	Error
			Benchmark 1			
3D	0.9063	%	1.7891	%	8.1549	%
LD1	0.9714	(7.18)	1.8232	(2.19)	8.1627	(0.09)
LD2	0.9064	(0.01)	1.7891	(0.00)	8.1549	(0.00)
LD3	0.9063	(0.00)	1.7891	(0.00)	8.1549	(0.00)
LD4	0.9063	(0.00)	1.7891	(0.00)	8.1549	(0.00)
			Benchmark 2			
3D	0.4911	%	0.6305	%	1.8283	%
LD1	0.6113	(24.5)	0.7279	(15.4)	1.8642	(1.96)
LD2	0.4912	(0.02)	0.6305	(0.00)	1.8283	(0.00)
LD3	0.4911	(0.00)	0.6305	(0.00)	1.8283	(0.00)
LD4	0.4911	(0.00)	0.6305	(0.00)	1.8283	(0.00)

Table 20 Comparison between 3D solutions versus ESL mixed models. $\bar{u}_z = U_z(100(E_T)_{skin}h^3/\bar{p}_z a^4)$ at the midsurface. Static analysis.

a/h	4	Error	10	Error	100	Error
			Benchmark 1			
3D	590.54	%	149.70	%	7.1881	%
EM4	114.14	(80.7)	24.337	(83.74)	5.7729	(19.7)
EMZ2	521.92	(11.6)	145.29	(2.95)	7.1901	(0.03)
EMZ3	516.45	(12.5)	144.88	(3.22)	7.1900	(0.03)
			Benchmark 2			
3D	1370.6	%	1260.3	%	149.51	%
EM4	128.09	(90.7)	26.955	(97.9)	5.7989	(96.1)
EMZ2	1055.2	(23.0)	996.89	(20.9)	145.28	(2.83)
EMZ3	1032.6	(24.7)	976.74	(22.5)	144.88	(3.10)

of the ESLM analysis to consider sandwich structures with soft cores. Two additional benchmarks, which refer to two additional values of the FCSR parameter, have been added to help explain the phenomenon.

Benchmark 4 (B4): Metallic faces and stiffer core than Nomex. This is a modification of Benchmark 1 in which the mechanical properties of the Nomex core are multiplied by a factor of 100. The Young moduli parameter ratios between the skins and faces are:

$$\mathrm{FCSR}_L = E_f/E_{cL} = 7.3E4, \quad \mathrm{FCSR}_z = E_f/E_{cz} = 9.62$$

All the data are reported in Table 24.

Benchmark 5 (B5): Metallic face and very soft core. This is an extreme modification of Benchmark 1 in which the mechanical properties of the Nomex core are divided by a factor of 10^{12}. Young moduli parameter ratios between the skins and faces are:

$$\mathrm{FCSR}_L = E_f/E_{cL} = 7.3E18, \quad \mathrm{FCSR}_z = E_f/E_{cz} = 9.62E14$$

All the data are reported in Table 25.

Figuers 13 and 14 show the in-plane stress distribution related to Benchmarks 1 and 2 and 4 and 5. 3D results are compared to a layerwise analysis and higher order theories. Benchmark 2 clearly shows the difficulties involved when using HOT to trace the stress distribution of sandwich plates with high FCSR, even when thin geometries are considered. Figure 15 shows that in the extreme case of very high FCSR (e.g., Benchmark 5), the shear stresses are very much concentrated in correspondence to the loaded skin; that is, if no material, or almost no core material, is placed between the two faces, there is no interaction between the loaded face (top

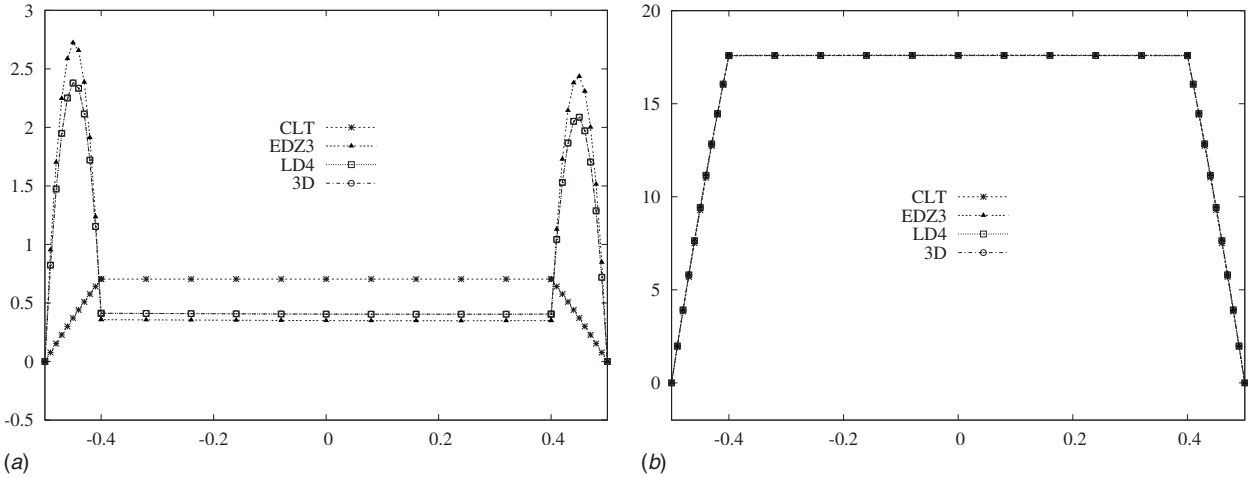

Fig. 12 Sandwich plate with a core in Nomex. Static analysis. σ_{xz} versus z. Comparison between 3D solutions, LW models, and HOT theories with MZZF. $a/h=4$ on the left. $a/h=100$ on the right.

Table 21 Comparison between 3D solutions versus layerwise mixed models. $\bar{u}_z = U_z(100(E_T)_{skin}h^3/\bar{p}_z a^4)$ at the midsurface. Static analysis.

a/h	4	Error	10	Error	100	Error
			Benchmark 1			
3D	590.54	%	149.70	%	7.1881	%
LM1	583.99	(1.11)	149.49	(0.14)	7.1881	(0.00)
LM2	590.55	(0.00)	149.70	(0.00)	7.1881	(0.00)
LM3	590.54	(0.00)	149.70	(0.00)	7.1881	(0.00)
LM4	590.54	(0.00)	149.70	(0.00)	7.1881	(0.00)
			Benchmark 2			
3D	1370.6	%	1260.3	%	149.51	%
LM1	1349.8	(1.52)	1257.3	(0.24)	149.50	(0.01)
LM2	1370.7	(0.01)	1260.3	(0.00)	149.51	(0.00)
LM3	1370.6	(0.00)	1260.3	(0.00)	149.51	(0.00)
LM4	1370.6	(0.00)	1260.3	(0.00)	149.51	(0.00)

Table 22 Comparison between 3D solutions versus layerwise mixed models. Static analysis. Transverse shear σ_{xz} stress at the midsurface.

a/h	4	Error	100	Error
		Benchmark 1		
3D	0.4053	%	17.594	%
LM1	–0.6433	(58.7)	17.291	(1.72)
LM2	0.4055	(0.05)	17.594	(0.00)
LM3	0.4049	(0.10)	17.594	(0.00)
LM4	0.4053	(0.00)	17.594	(0.00)
		Benchmark 2		
3D	0.0094	%	15.743	%
LM1	0.0094	(0.00)	15.743	(0.00)
LM2	0.0093	(1.06)	15.743	(0.00)
LM3	0.0099	(5.32)	15.743	(0.00)
LM4	0.0094	(0.00)	15.743	(0.00)

Table 23 Comparison between 3D solutions versus layerwise mixed models. Free vibration problem. Fundamental frequency: $\bar{\omega} = \omega\sqrt{a^4(\rho)_{skin}/(E_T)_{skin}h^2}$. $m,n=1$. Comparison between 3D solutions versus layerwise mixed models.

a/h	4	Error	10	Error	100	Error
			Benchmark 1			
3D	0.9063	%	1.7891	%	8.1549	%
LM1	0.9043	(0.22)	1.7882	(0.05)	8.1549	(0.00)
LM2	0.9063	(0.00)	1.7891	(0.00)	8.1549	(0.00)
LM3	0.9063	(0.00)	1.7891	(0.00)	8.1549	(0.00)
LM4	0.9063	(0.00)	1.7891	(0.00)	8.1549	(0.00)
			Benchmark 2			
3D	0.4911	%	0.6305	%	1.8283	%
LM1	0.4917	(0.12)	0.6304	(0.01)	1.8283	(0.00)
LM2	0.4911	(0.00)	0.6305	(0.00)	1.8283	(0.00)
LM3	0.4911	(0.00)	0.6305	(0.00)	1.8283	(0.00)
LM4	0.4911	(0.00)	0.6305	(0.00)	1.8283	(0.00)

skin) and the unloaded one (bottom skin). In other words the kinematics of the two faces are completely independent. These independent kinematics can only be considered by using a LW description; no HOT is able to describe such independent kinematics.

The results of the dynamic cases are given in Tables 26 and 27. CLT, ED2, EDZ2, and LD2 results are compared. The complete set of frequencies associated with the model is listed. The number of frequencies for fixed values of m and n is, in fact, only related to the degrees of freedom of the employed plate theories. Benchmarks 1 and 5 are compared in these two tables. The capability of

Table 24 Benchmark 4. Elastic and geometrical properties of a sandwich plate with increased core stiffness.

Properties	Layers 1–3 (Al 2024)
E (GPa)	73
ν	0.34
G (GPa)	27.239
ρ (kg/m^3)	2800
$h_1=h_3$ (m)	0.1
$a=b$	4, 10, 100, 1000
	Layer 2 (Nomex: modulus multiply by 100)
$E_L=E_T$ (MPa)	1
E_z (MPa)	7585
ν	0.01
G (MPa)	2250
ρ (kg/m^3)	3200
h_2 (m)	0.8
$a=b$	4, 10, 100, 1000

Table 25 Benchmark 5. Elastic and geometrical properties of a sandwich plate with high reduced core stiffness.

Properties	Layers 1–3 (Al 2024)
E (GPa)	73
ν	0.34
G (GPa)	27.239
ρ (kg/m^3)	2800
$h_1=h_3$ (m)	0.1
$a=b$	4, 10, 100, 1000
	Layer 2 (Nomex: modulus divided by 10^{12})
$E_L=E_T$ (μPa)	0.01
E_z (μPa)	75.85
ν	0.01
G (μPa)	22.5
ρ (kg/m^3)	3.2×10^{-11}
h_2 (m)	0.8
$a=b$	4, 10, 100, 1000

the LW analysis to describe the independent kinematics of the two layers is clearly shown. In the extreme case of Benchmark 5, double values of each frequencies are, in fact, found when using the LW analysis. These values are related to the two "independent" faces, *which vibrate as two independent plates*. Such behavior cannot be captured by any HOT, which, by definition, considers the sandwich panel as a single "equivalent" plate. As final results, Figs. 16 and 17 show the stiffness matrix related to ESLM and LW analyses. The resulting full linear systems of algebraic equations are written for the ED2 and LD2 cases. Significant changes in the stiffness of the core (which occurs when the core stiffness between Benchmarks 1 and 5 is reduced) do not introduce any modification of the stiffness coefficients in Fig. 16. On the contrary, the LW analysis in Fig. 17 clearly shows that in the case of Benchmark 5, the two faces are completely uncoupled in the resulting linear system of algebraic equations. As a consequence, if the load is applied in correspondence to the top layer, there is no way of transferring that load effect to the bottom face since there are only zeros in-between in the stiffness matrix.

8 Conclusions

A numerical assessment of classical, higher order, zigzag, layerwise, and mixed theories has been considered in this paper through a comparison of the results of bending and vibration of

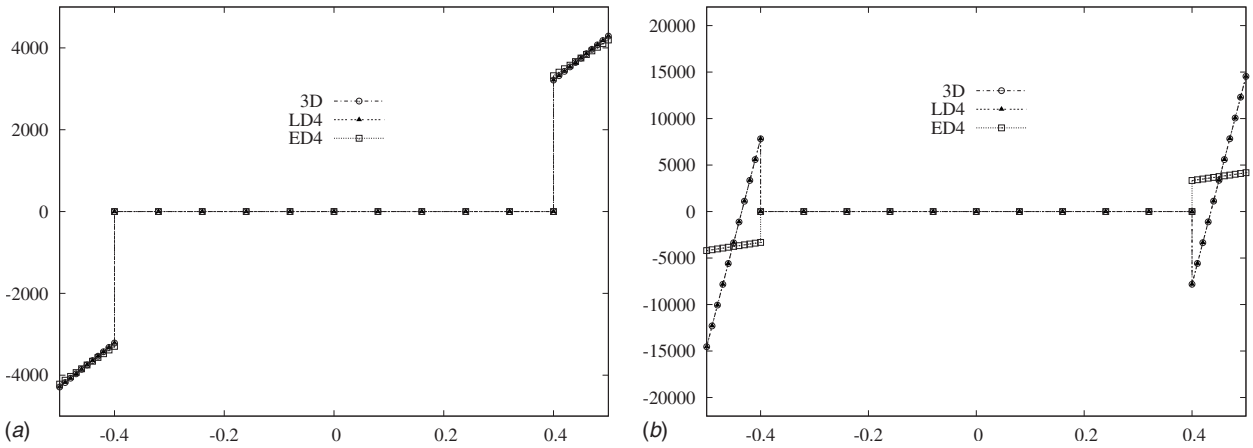

Fig. 13 In-plane stress evaluation Benchmark 1 (left) and Benchmark 2 (right). Sandwich plate with a core in Nomex. Static analysis. σ_{xx} versus z. Comparison between 3D solutions, HOT, and LW theories. Thin plate case $a/h=100$.

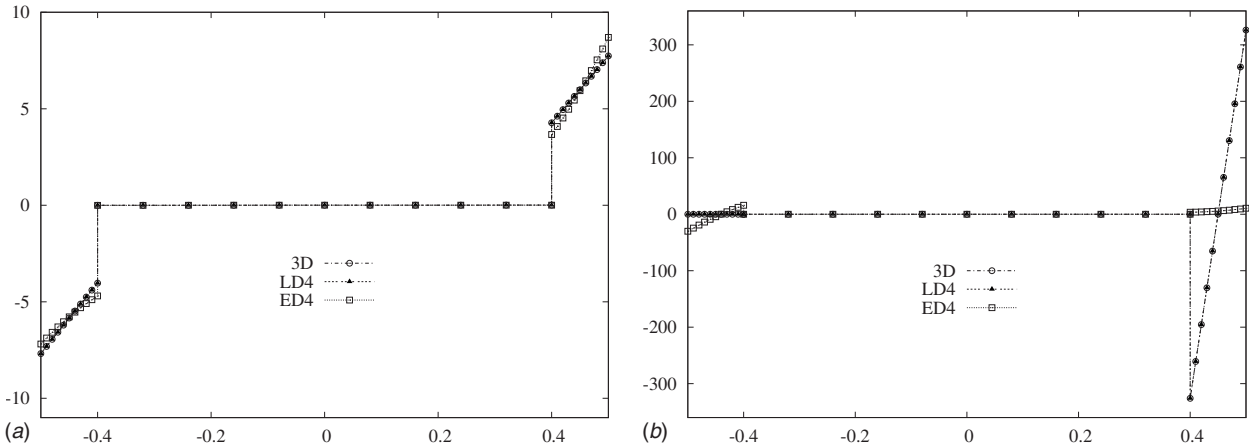

Fig. 14 In-plane stress evaluations. Benchmark 4 (left) versus Benchmark 5 (right). σ_{xx} versus z. Comparison between 3D solutions, HOT, and LW theories. Thick plate case $a/h=4$.

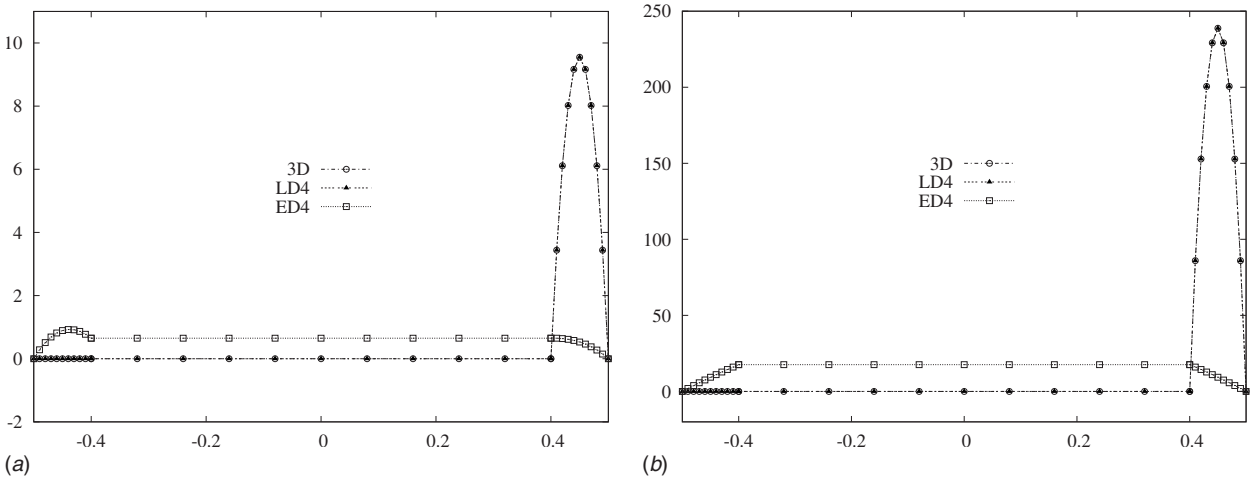

Fig. 15 Benchmark 5. Sandwich plate with high reduced core stiffness. Static analysis. σ_{xz} versus z. Comparison between 3D solutions, HOT, and LW theories. $a/h=4$ on the left. $a/h=100$ on the right.

Table 26 Benchmark 1. Sandwich plate with a core in Nomex. Free vibration problem. $\bar{\omega}=\omega\sqrt{a^4(\rho)_{skin}/(E_T)_{skin}h^2}$. $m,n=1$. $a/h=100$.

Frequency	CLT	ED2	EDZ2	LD2
ω_1	265.39	265.39	265.39	8.1549
ω_2	462.24	461.81	462.24	265.38
ω_3	9.2551	9.2473	8.1541	462.20
ω_4		27,281	2192.4	911.85
ω_5		131,253	989.55	989.47
ω_6		131,252	911.86	2192.5
ω_7		13,499	420,391	6612.8
ω_8		266,281	131,253	6613.6
ω_9		13,491	131,252	16,643
ω_{10}			266,281	206,921
ω_{11}			207,001	209,234
ω_{12}			207,000	206,920
ω_{13}				209,235
ω_{14}				928,590
ω_{15}				943,779
ω_{16}				420,227
ω_{17}				424,896
ω_{18}				457,217
ω_{19}				464,707
ω_{20}				457,216
ω_{21}				464,706

Table 27 Benchmark 5. Sandwich plate with high reduced core stiffness. Free vibration problem. $\bar{\omega}=\omega\sqrt{a^4(\rho)_{skin}/(E_T)_{skin}h^2}$. $m,n=1$. $a/h=100$.

Frequency	CLT	ED2	EDZ2	LD2
ω_1	271.39	271.39	17.388	0.6059
ω_2	472.43	472.41	271.39	0.6059
ω_3	9.4628	27,514	472.43	271.39
ω_4		211,953	0.7064	271.39
ω_5		9.4571	472.78	472.43
ω_6		211,952	429,769	472.43
ω_7		13,557	211,953	6491.9
ω_8		13,549	271.39	6491.5
ω_9		430,475	430,475	16,336
ω_{10}			211,952	960,992
ω_{11}			211,605	960,992
ω_{12}			211,604	211,605
ω_{13}				211,605
ω_{14}				211,605
ω_{15}				211,604
ω_{16}				429,772
ω_{17}				429,763
ω_{18}				473,162
ω_{19}				473,162
ω_{20}				473,161
ω_{21}				473,161

sandwich flat panels. Several benchmarks, related to different values of the mechanical properties between the face and core (FCSR) have been analyzed. The following main conclusions can be drawn.

1. It appears clear that there are two sources of error in the 2D modeling of sandwich structures:
   (a) the first is related to the length-to-thickness ratio (LTR),
   (b) the second is related to the stiffness ratio between the skins and core (FCSR).
2. The numerical investigation has shown that the first error can be somewhat contrasted by the use of refined plate models, while the second source of error can only be contrasted by the use of layerwise kinematics. A summary is given in Table 28, which shows these errors for transverse displacement in the midplane. An additional mixed parameter R =FCSR/LTR has been introduced in this table, which tries

$$\begin{bmatrix} 2.7E^7 & 1.7E^7 & 0.0 & 0.0 & 0.0 & -3.6E^8 & 5.6E^6 & 3.4E^6 & 0.0 \\ 1.7E^7 & 2.7E^7 & 0.0 & 0.0 & 0.0 & -3.6E^8 & 3.4E^6 & 5.6E^6 & 0.0 \\ 0.0 & 0.0 & 1.1E^7 & 1.7E^8 & 1.7E^8 & 0.0 & 0.0 & 0.0 & 2.2E^6 \\ 0.0 & 0.0 & 1.7E^8 & 5.5E^9 & 3.4E^6 & 0.0 & 0.0 & -1E^{-10} & -1.1E^8 \\ 0.0 & 0.0 & 1.7E^8 & 3.4E^6 & 5.5E^9 & 0.0 & -1E^{-10} & 0.0 & -1.1E^8 \\ -3.6E^8 & -3.6E^8 & 0.0 & 0.0 & 0.0 & 2.2E^{10} & -4.3E6 & -4.3E^6 & 0.0 \\ 5.6E^6 & 3.4E^6 & 0.0 & 0.0 & -1E^{-10} & -4.3E^6 & 4.4E^9 & 7.1E^5 & 0.0 \\ 3.4E^6 & 5.6E^6 & 0.0 & -1E^{-10} & 0.0 & -4.3E^6 & 7.1E^5 & 4.4E^9 & 0.0 \\ 0.0 & 0.0 & 2.2E^6 & -1.1E^8 & -1.1E^8 & 0.0 & 0.0 & 0.0 & 1.8E^{10} \end{bmatrix} \begin{Bmatrix} u_t \\ v_t \\ w_t \\ u_2 \\ v_2 \\ w_2 \\ u_b \\ v_b \\ w_b \end{Bmatrix} = \begin{Bmatrix} 0 \\ 0 \\ p \\ 0 \\ 0 \\ 0 \\ 0 \\ 0 \\ 0 \end{Bmatrix}$$

(*a*)

$$\begin{bmatrix} 2.7E^7 & 1.7E^7 & 0.0 & 0.0 & 0.0 & -3.6E^8 & 5.6E^6 & 3.4E^6 & 0.0 \\ 1.7E^7 & 2.7E^7 & 0.0 & 0.0 & 0.0 & -3.6E^8 & 3.4E^6 & 5.6E^6 & 0.0 \\ 0.0 & 0.0 & 1.1E^7 & 1.7E^8 & 1.7E^8 & 0.0 & 0.0 & 0.0 & 2.2E^6 \\ 0.0 & 0.0 & 1.7E^8 & 5.5E^9 & 3.4E^6 & 0.0 & 0.0 & -1E^{-10} & -1.1E^8 \\ 0.0 & 0.0 & 1.7E^8 & 3.4E^6 & 5.5E^9 & 0.0 & -1E^{-10} & 0.0 & -1.1E^8 \\ -3.6E^8 & -3.6E^8 & 0.0 & 0.0 & 0.0 & 2.2E^{10} & -4.3E6 & -4.3E^6 & 0.0 \\ 5.6E^6 & 3.4E^6 & 0.0 & 0.0 & -1E^{-10} & -4.3E^6 & 4.4E^9 & 7.1E^5 & 0.0 \\ 3.4E^6 & 5.6E^6 & 0.0 & -1E^{-10} & 0.0 & -4.3E^6 & 7.1E^5 & 4.4E^9 & 0.0 \\ 0.0 & 0.0 & 2.2E^6 & -1.1E^8 & -1.1E^8 & 0.0 & 0.0 & 0.0 & 1.8E^{10} \end{bmatrix} \begin{Bmatrix} u_t \\ v_t \\ w_t \\ u_2 \\ v_2 \\ w_2 \\ u_b \\ v_b \\ w_b \end{Bmatrix} = \begin{Bmatrix} 0 \\ 0 \\ p \\ 0 \\ 0 \\ 0 \\ 0 \\ 0 \\ 0 \end{Bmatrix}$$

(*b*)

Fig. 16 Comparison Benchmark 1 and Benchmark 5. Sandwich plate with a core in Nomex (on the top) and with high reduced core stiffness (on the bottom). ED2 theory. $a/h=100$. Static case.

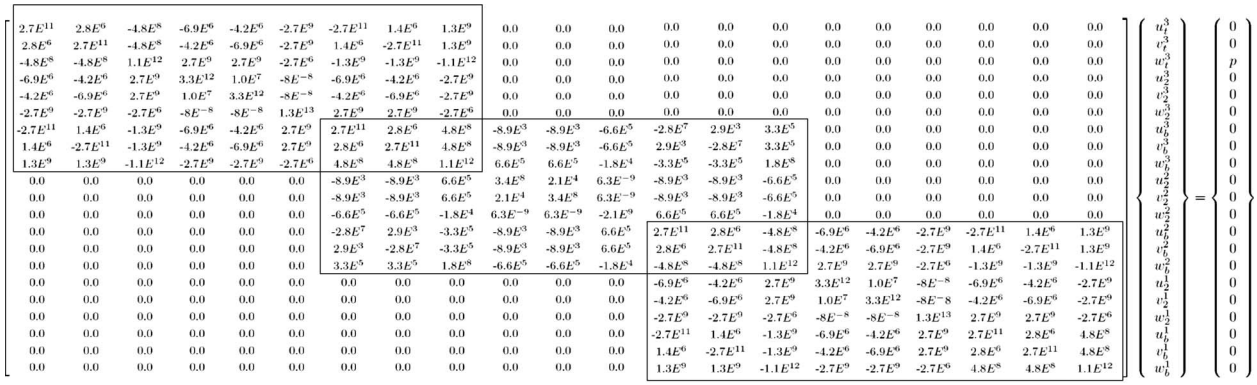

(*a*)

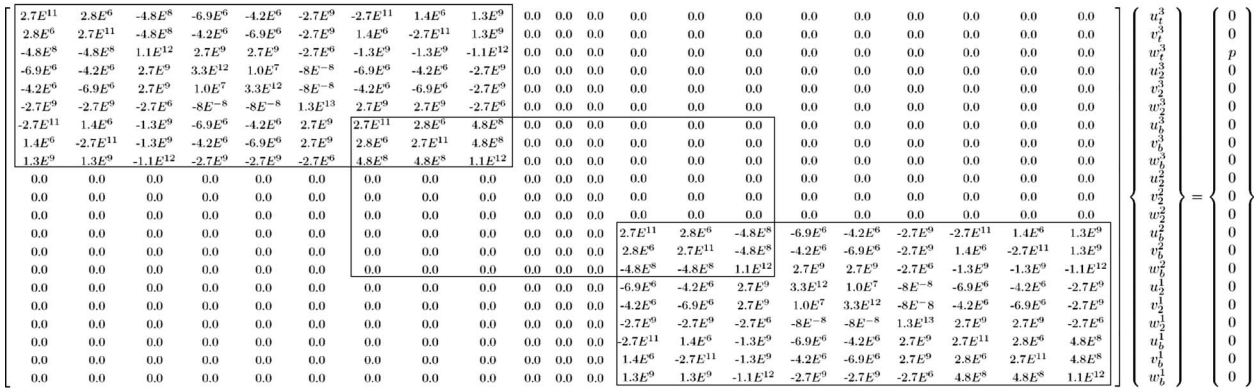

(*b*)

Fig. 17 Comparison of Benchmark 1 and Benchmark 5. Sandwich plate with a core in Nomex (on the top) and with high reduced core stiffness (on the bottom). LD2 theory. $a/h=100$. Static case.

Table 28 Error in percentage (%) with respect to a 3D solution for a static analysis of the sandwich plate. $\bar{u}_z = U_z(100(E_T)_{skin}h^3/p_z a^4)$ at the midsurface is given for the 3D cases. R is the ratio R=FCSR/LTR.

FCSR	LTR	4	10	100	1000
	R	18.25	7.3	0.73	0.073
	3D ($\bar{w}$)	0.1982	0.1901	0.1885	0.1885
7.3×10^1	ED4	1.61	0.79	1.22	1.22
	EMZC3	1.66	0.74	1.17	1.17
	LD1	1.06	0.16	0.05	0.05
	LD4	0.00	0.00	0.00	0.00
	XXX		to be filled in		
	R	1825	730	73	7.3
	3D ($\bar{w}$)	15.483	7.0360	5.4424	5.4240
7.3×10^4	ED4	7.45	3.70	1.58	1.50
	EMZC3	0.60	4.06	5.56	5.62
	LD1	0.91	0.23	0.14	0.23
	LD4	0.00	0.00	0.00	0.00
	XXX		to be filled in		
	R	1825×10^3	73×10^4	73×10^3	73×10^2
	3D ($\bar{w}$)	590.54	149.70	7.1881	5.5980
7.3×10^6	ED4	82.8	85.2	20.0	0.25
	EMZC3	12.5	3.22	0.03	0.01
	LD1	14.3	3.93	0.19	0.35
	LD4	0.00	0.00	0.00	0.00
	XXX		to be filled in		
	R	1825×10^5	73×10^6	73×10^5	73×10^4
	3D ($\bar{w}$)	1370.6	1260.3	149.51	7.1901
7.3×10^8	ED4	91.8	98.1	96.1	22.3
	EMZC3	24.7	22.5	3.10	0.01
	LD1	27.4	25.2	3.82	0.39
	LD4	0.00	0.00	0.00	0.00
	XXX		to be filled in		

to relate the errors due to mechanics and geometries. The obtained errors for the various R-values once again demonstrate the independence between the two parameters LTR and FCSR.

3. The use of Murakami's zigzag function appears extremely convenient. Its use would seem preferable to other ESLM refined kinematics with only displacement unknowns.
4. CLT and FSDT cannot be effectively used for the analysis of sandwich structures.
5. The accuracy of various theories seems to be very much subordinate to the considered variables (stress, displacement components and circular frequency) as well as to the location in the thickness direction.

The authors hope that this work will be of some help to those specialists who model sandwich structures as desk-beds to assess improved theories in a more complete and exhaustive way than in the past. In particular scientists who propose "new improved theories" are encouraged to consider Table 28 and to perform a complete assessment by filling the remaining blank row.

The numerical analysis presented in this work has been limited to orthotropic plates with simply supported boundary conditions, loaded by the transverse distribution of bisinusoidal pressure. Additional investigations are required to extend the obtained conclusions to more general boundary conditions, materials, and loading, including localized ones. Finite element methods could be conveniently used for this purpose. These analyses could be the subject of future works.

Acknowledgment

This work has been carried out in the framework of the STREP EU project CASSEM under Contract No. NMP-CT-2005-013517.

References

[1] Plantema, F. J., 1966, *Sandwich Construction*, Wiley, New York.
[2] Allen, H. G., 1969, *Analysis and Design of Structural Sandwich Panels*, Pergamon, Oxford.
[3] Zenkert, D., 1995, *An Introduction to Sandwich Structures*, Chamelon, Oxford.
[4] Bitzer, T. N., 1997, *Honeycomb Technology*, Chapman and Hall, London.
[5] Vinson, J. R., 1999, *The Behavior of Sandwich Structures of Isotropic and Composite Materials*, Technomic, Lancaster, PA.
[6] Marshall, A. C., 1990, *Core Composite and Sandwich Structures* (International Encyclopedia of Composites), Vol. I, S. M. Lee, ed., VCH, New York, pp. 488–607.
[7] Corden, J., 1995, *Honeycomb Structures* (ASM Handbook I: Composites), J. R. Davies, ed., American Society of Metals, Metals Park, OH, pp. 721–728.
[8] Pagano, N. J., 1970, "Exact Solutions for Rectangular Bidirectional Composites and Sandwich Plates," J. Compos. Mater., **4**, pp. 20–34.
[9] Dundrova, V., 1966, "Stress and Strain Analysis of Simply Supported Non-Homogenous Rectangular Plates on the Basis of Lamé Equations," *Theory of Plates and Shells*, Vydavatesstvo Slovenskej Akademie vied, Bratislava.
[10] Meyer-Piening, H. R., 2004, "Application of the Elasticity Solution to Linear Sandwich Beams, Plates and Shells Analysis," J. Sandwich Struct. Mater., **6**, pp. 295–312.
[11] Demasi, L., 2007, "Three Dimensional Closed Form Solution and Exact Thin Plate Theories for Isotropic Plates," Compos. Struct., **80**, pp. 183–195.
[12] Cauchy, A. L., 1828, "Sur l'equilibre et le mouvement d'une plaque solide," Exercises Math., **3**, pp. 328–355.
[13] Poisson, S. D., 1829, "Memoire sur l'equilibre et le mouvement des corps elastique," Mem. Acad. Sci. Inst. Fr., **8**, p. 357–570.
[14] Kirchhoff, G., 1850, "Uber das Gleichgewicht und die Bewegung einer elastischen Scheibe," J. Reine Angew. Math., **40**, pp. 51–88.
[15] Love, A. E. H., 1927, *The Mathematical Theory of Elasticity*, 4th ed., Cambridge University Press, Cambridge.
[16] Reissner, E., 1945, "The Effect of Transverse Shear Deformation on the Bending of Elastic Plates," ASME J. Appl. Mech., **12**, pp. 69–76.
[17] Mindlin, R. D., 1951, "Influence of Rotatory Inertia and Shear in Flexural Motions of Isotropic Elastic Plates," ASME J. Appl. Mech., **18**, pp. 1031–1036.
[18] Carrera, E., 1995, "A Class of Two-Dimensional Theories for Anisotropic Multilayered Plates Analysis," Atti Accad. Sci. Torino Mem. Sci. Fis., **19–20**, pp. 1–39.
[19] Lekhnitskii, S. G., 1968, *Anisotropic Plates*, 2nd ed., S. W. Tsai, translator, Gordon and Breach, New York.
[20] Ambartsumian, S. A., 1961, *Theory of Anisotropic Shells*, translated from Russian, NASA TTF-18, Fizmatzig, Moskwa.
[21] Ambartsumian, S. A., 1969, *Theory of Anisotropic Plates*, J. E. Ashton, T. Cheron tanslator, Technomic Publishing Company, Moskwa.
[22] Ambartsumian, S. A., 1991, *Fragments of the Theory of Anisotropic Shells*, World Scientific, Singapore.
[23] Librescu, L., 1975, *Elasto-Statics and Kinetics of Anisotropic and Heterogeneous Shell-Type Structures*, Noordhoff, Leyden, The Netherlands.
[24] Reddy, J. N., 1997, *Mechanics of Laminated Composite Plates, Theory and Analysis*, CRC, Boca Raton, FL.
[25] Ambartsumian, S. A., 1962, "Contributions to the Theory of Anisotropic Layered Shells," Appl. Mech. Rev., **15**, pp. 245–249.
[26] Habip, L. M., 1964, "A Review of Recent Russian Work on Sandwich Structures," Int. J. Mech. Sci., **6**, pp. 483–487.
[27] Habip, L. M., 1965, "A Review of Recent Work on Multilayered Structures," Int. J. Mech. Sci., **8**, pp. 589–583.
[28] Grigolyuk, E. I., and Kogan, F. A., 1972, "State of Art of the Theory of Multilayer Shells," Appl. Mech. Rev., **15**, pp. 245–249.
[29] Sun, C. T., and Whitney, J. M., 1973, "On the Theories for the Dynamic Response of Laminated Plates," Am. Inst. of Aeronaut. Astronaut. J., **11**, pp. 372–398.
[30] Leissa, A. W., 1987, "A Review of Laminated Composite Plate Buckling," Appl. Mech. Rev., **15**, pp. 245–249.
[31] Librescu, L., and Reddy, J. N., 1987, "A Critical Review and Generalization of Transverse Shear Deformable Anisotropic Plates," *Euromech Colloquium, 219, Refined Dynamical Theories of Beams, Plates and Shells and Their Applications*, Kassel, September 1986, I. Elishakoff and H. Irretier, eds., Springer, Berlin, pp. 32–43.
[32] Grigolyuk, E. I., and Kulikov, G. M., 1988, "General Directions of the Development of Theory of Shells," Mekh. Kompoz. Mater., **24**, pp. 287–298.
[33] Kapania, R. K., and Raciti, S., 1989, "Recent Advances in Analysis of Laminated Beams and Plates," Am. Inst. of Aeronaut. Astronaut. J., **27**, pp. 923–946.
[34] Kapania, R. K., 1989, "A Review on the Analysis of Laminated Shells," ASME J. Pressure Vessel Technol., **111**, pp. 88–96.
[35] Vasiliev, V. V., and Lur'e, S. A., 1992, "On Refined Theories of Beams, Plates and Shells," J. Compos. Mater., **26**, pp. 422–430.
[36] Noor, A. K., and Burton, W. S., 1989, "Assessment of Shear Deformation Theories for Multilayered Composite Plates," Appl. Mech. Rev., **41**, pp. 1–18.
[37] Noor, A. K., and Burton, W. S., 1990, "Assessment of Computational Models for Multilayered Composite Shells," Appl. Mech. Rev., **43**, pp. 67–97.
[38] Burton, S., and Noor, A. K., 1995, "Assessment of Computational Model for Sandwich Panels and Shells," Comput. Methods Appl. Mech. Eng., **124**, pp. 125–151.
[39] Noor, A. K., Burton, S., and Bert, C. W., 1996, "Computational Model for Sandwich Panels and Shells," Appl. Mech. Rev., **49**, pp. 155–199.
[40] Jemielita, G., 1990, "On Kinematical Assumptions of Refined Theories of Plates: A Survey," ASME J. Appl. Mech., **57**, pp. 1080–1091.
[41] Reddy, J. N., and Robbins, D. H., 1994, "Theories and Computational Models for Composite Laminates," Appl. Mech. Rev., **47**, pp. 147–165.
[42] Lur'e, S. A., and Shumova, N. P., 1996, "Kinematic Models of Refined Theories Concerning Composite Beams Plates and Shells," Int. Appl. Mech., **32**, pp. 422–430.
[43] Grigorenko, Ya. M., 1996, "Approaches to Numerical Solution of Linear and Nonlinear Problems in Shell Theory in Classical and Refined Formulations," Int. Appl. Mech., **32**, pp. 409–442.
[44] Grigorenko, Ya. M., and Vasilenko, A. T., 1997, "Solution of Problems and Analysis of the Stress Strain State of Non-Uniform Anisotropic Shells (Survey)," Int. Appl. Mech., **33**, pp. 851–880.
[45] Altenbach, H., 1998, "Theories for Laminated and Sandwich Plates: A Review," Int. Appl. Mech., **34**, pp. 243–252.
[46] Librescu, L., and Hause, T., 2000, "Recent Developments in the Modeling and Behaviors of Advanced Sandwich Constructions: A Survey," Compos. Struct., **48**, pp. 1–17.
[47] Vinson, J. R., 2001, "Sandwch Structures, Applied Mechanics Reviews," Appl. Mech. Rev., **54**, pp. 201–214.
[48] Carrera, E., 2001, "Developments, Ideas and Evaluations Based Upon the Reissner's Mixed Theorem in the Modeling of Multilayered Plates and Shells," Appl. Mech. Rev., **54**, pp. 301–329.
[49] Qatu, M. S., 2002, "Recent Research Advances in the Dynamic Behavior of Shells: 1989-2000. Part 1: Laminated Composite Shells," Appl. Mech. Rev., **55**, pp. 325–330.
[50] Hohe, J., and Becker, W., 2002, "Effective Stress-Strain Relations for Two-Dimensional Cellular Sandwich Core: Homogenization, Material Models, and Properties," Appl. Mech. Rev., **55**, pp. 61–87.
[51] Hohe, J., and Librescu, L., 2004, "Advances in the Structural Modeling of Elastic Sandwich Panels," Mech. Adv. Mater. Struct., **11**, pp. 395–424.
[52] Carrera, E., 2003, "A Historical Review of Zig-Zag Theories for Multilayered Plates and Shell," Appl. Mech. Rev., **56**, pp. 290–309.
[53] Lekhnitskii, S. G., 1935, "Strength Calculation of Composite Beams," Vestn. Inzh. Tekh.. (9).
[54] Ambartsumian, S. A., 1958, "On a Theory of Bending of Anisotropic Plates," Izv. Akad. Nauk SSSR, Otd. Tekh. Nauk. (4).
[55] Ambartsumian, S. A., 1958, "On a General Theory of Anisotropic Shells," Prikl. Mat. Mekh., **22**(2), pp. 226–237.
[56] Reissner, E., 1984, "On a Certain Mixed Variational Theory and a Proposed Applications," Int. J. Numer. Methods Eng., **20**, pp. 1366–1368.
[57] Frostig, Y., 1999, "Bending of Curved Sandwich Panels With Transversely Flexible Core: Closed Form Higher-Order Theory," J. Sandwich Struct. Mater., **1**, pp. 4–41.

[58] Frostig, Y., and Rabinovich, O., 2000, "Behavior of Unidirectional Sandwich Panels With a Multi-Skin Construction or a Multilayered Core Layout-Higher-Order Approach," J. Sandwich Struct. Mater., **2**, pp. 181–213.
[59] Rabinovich, O., and Frostig, Y., 2001, "High-Order Analysis of Unidirectional Sandwich Panels With Flat and Generally Curved Faces and Soft Core," J. Sandwich Struct. Mater., **3**, pp. 89–116.
[60] Frostig, Y., and Thomsen, O. T., 2005, "Localized Effects in the Nonlinear Behavior of Sandwich Panels With a Transversely Flexible Core," Journal of Sandwich and Structures and Materials, **7**, pp. 53–77.
[61] Frostig, Y., and Thomsen, O. T., 2006, "Localized Effects Near Non-Vertical Core Junctions In Sandwich Panels: A High-Order Approach," J. Sandwich Struct. Mater., **8**, pp. 125–156.
[62] Pantano, A., and Averill, R. C., 2000, "A 3D Zig-Zag Sub-Laminate Model for the Analysis of Thermal Stresses in Laminated Composite and Sandwich Plate," Journal of Sandwich and Structures and Materials, **2**, pp. 288–312.
[63] Swanson, S. R., 2000, "Response of Orthotropic Sandwich Plates to Concentrated Loadings," J. Sandwich Struct. Mater., **2**, pp. 270–287.
[64] Swanson, S. R., and Kim, J., 2000, "Comparison of Higher Order Theory for Sandwich Beams With Finite Element and Elasticity Analysis," J. Sandwich Struct. Mater., **2**, pp. 33–49.
[65] Whitney, J. M., 2001, "A Local Model for Bending of Weak Core Sandwich Plates," J. Sandwich Struct. Mater., **3**, pp. 269–288.
[66] Pagano, J. N., 1978, "Stress Fields in Composite Laminates," Int. J. Solids Struct., **14**, pp. 385–400.
[67] Liu, Q., and Zhao, Y., 2001, "Prediction of Natural Frequencies of a Sandwich Panel Using Thick Plate Theories," J. Sandwich Struct. Mater., **3**, pp. 289–319.
[68] Birman, V., and Bert, C. W., 2001, "On the Choice of Shear Correction Factor in Sandwich Structures," J. Sandwich Struct. Mater., **4**, pp. 83–98.
[69] Matsunaga, H., 2002, "Assessment of a Global Higher-Order Deformation Theory for Laminated Composite and Sandwich Plates," Comput. Struct., **56**, pp. 279–291.
[70] Topdar, P., Sheikh, A. H., and Dhang, N., 2003, "Finite Element Analysis of Composite and Sandwich Plates Using a Continuous Interlaminar Shear Stress Model," J. Sandwich Struct. Mater., **5**, pp. 207–229.
[71] Lyckegaard, A., and Thomsen, O. T., 2004, "High Order Analysis of Junction Between Straight and Curved Panels," J. Sandwich Struct. Mater., **6**, pp. 497–529.
[72] Garg, A. K., Khare, R. K., Kant, T., 2005, "Free Vibration Analysis of Skew Fiber-Reinforced Composite and Sandwich Laminates Using a Shear Deformable Finite Element Model," J. Sandwich Struct. Mater., **8**, pp. 33–53.
[73] Malekzadeh, K., Khalili, M. R., and Mittal, R. K., 2005, "Local and Global Damped Vibrations of Plates With Viscoelastic Soft Flexible Core," Journal of Sandwich and Structures and Materials, **7**, pp. 431–456.
[74] Roque, C. M. C., Ferreira, A. J. A., and Jorge, R. M. N., 2006, "Free Vibration Analysis of Composite and Sandwich Plate by Trigonometric Layer-Wise Deformation Theory and Radial Basis Function," J. Sandwich Struct. Mater., **8**, pp. 497–515.
[75] Hu, H., Beluouettra, S., Daya, E. M., and Potier-Ferry, M., 2006, "Evaluation of Kinematic Formulations for Viscoelastically Damped Sandwich Beam Modeling," J. Sandwich Struct. Mater., **8**, pp. 477–495.
[76] Carrera, E., 1998, "Layer-Wise Mixed Models for Accurate Vibration Analysis of Multilayered Plates," ASME J. Appl. Mech., **65**, pp. 820–828.
[77] Carrera, E., Demasi, L., and Manganello, M., 2002, "Assessment of Plate Elements on Bending and Vibrations of Composite Structures," Mech. Adv. Mater. Struct., **9**, pp. 333–357.
[78] Carrera, E., and Demasi, L., 2002, "Multilayered Finite Plate Element Based on Reissner's Mixed Variational Theorem. Part I: Theory," Int. J. Numer. Methods Eng., **55**, pp. 191–231.
[79] Carrera, E. and Demasi, L., 2002, "Multilayered Finite Plate Element Based on Reissner's Mixed Variational Theorem. Part II: Numerical Analysis," Int. J. Numer. Methods Eng., **55**, pp. 253–291.
[80] Carrera, E., 2003, "Theories and Finite Elements for Multilayered Plates and Shells: A Unified Compact Formulation With Numerical Assessment and Benchmarking," Arch. Comput. Methods Eng., **10**, pp. 215–296.
[81] Carrera, E., and Brischetto, S., 2008, "Analysis of Thickness Locking in Classical, Refined and Mixed Multilayered Plate Theories," Compos. Struct., **82**, pp. 549–562.
[82] Murakami, H., 1986, "Laminated Composite Plate Theory With Improved In-Plane Responses," ASME J. Appl. Mech., **53**, pp. 661–666.

Erasmo Carrera. *After earning two degrees (Aeronautics, 1986 and Aerospace Engineering, 1988) in the Politecnico di Torino, Erasmo Carrera received his Ph.D. degree in Aerospace Engineering in 1991 at the Politecnico di Milano–Politecnico di Torino–Universitá di Pisa. He began working as a Researcher at the Department of Aerospace of Politecnico di Torino in 1992, holding courses on Missiles and Aerospace Structure Design, Plates and Shells and Finite Element Method, and since 2000 he is Associate Professor of Aerospace Structures and Aeroelasticity. He visited twice the Institute für Statik und Dynamik, Universität Stuttgart, the first time as a Ph.D. student (six months in 1991) and then as a Visiting Scientist under a GKKS grant (18 months in 1995–1996). In the summer of 1996, he was a Visiting Professor at ESM Department of Virginia Tech. His main research topics are composite materials, finite elements, plates and shells, postbuckling and stability by FEM, smart structures, thermal stress, aeroelasticity, multibody dynamics, and design and analysis of nonclassical lifting systems. He is an author of more than 80 articles on these topics, many of which have been published in international journals. He serves as a referee for many journals such as Applied Mechanics Reviews, AIAA Journal, Journal of Sound and Vibration, International Journal of Solids and Structures, and International of Numerical Methods in Engineering and as contributing editor for Mechanics of Advanced Materials and Structures.*

Salvatore Brischetto. *After earning the degree in Aeronautics and Space Engineering (2005) in the Politecnico di Torino, Salvatore Brischetto began his Ph.D. in Aerospace Engineering (2006) in co-tutoring between the Politecnico di Torino and the Laboratoire de Mécanique de Paris X, Université Paris X Nanterre. His main research topics are composite materials, smart structures, analytical and numerical two-dimensional models for multilayered plates and shells, and multifield problems for multilayered structures. He is author of more than 20 articles on these topics, many of which have been published in international journals.*